# 4-(3-Aminoazetidin-1-yl)pyrimidin-2-amines as High-Affinity Non-imidazole Histamine H₃ Receptor Agonists with in Vivo Central Nervous System Activity

Gábor Wágner,[†] Tamara A. M. Mocking,[†] Marta Arimont,[†] Gustavo Provensi,[‡] Barbara Rani,[§] Bruna Silva-Marques,[‡,∥] Gniewomir Latacz,[⊥] Daniel Da Costa Pereira,[†] Christina Karatzidou,[†] Henry F. Vischer,[†] Maikel Wijtmans,[†] Katarzyna Kieć-Kononowicz,[⊥] Iwan J. P. de Esch,[†] and Rob Leurs*,[†]

[†]Amsterdam Institute for Molecules, Medicines and Systems (AIMMS), Division of Medicinal Chemistry, Faculty of Science, Vrije Universiteit Amsterdam, De Boelelaan 1108, 1081 HZ Amsterdam, The Netherlands

[‡]Department of Neuroscience, Psychology, Drug Research and Child Health, Section of Pharmacology and Toxicology and [§]Department of Health Sciences, University of Florence, Viale G. Pieraccini 6, CAP 50139 Florence, Italy

[∥]Department of Physiotherapy, Federal University of São Carlos, Washington Luís, km 235, SP-310 São Carlos, Brazil

[⊥]Department of Technology and Biotechnology of Drugs, Medical College, Jagiellonian University, Medyczna 9, PL 30-688 Cracow, Poland

S *Supporting Information*
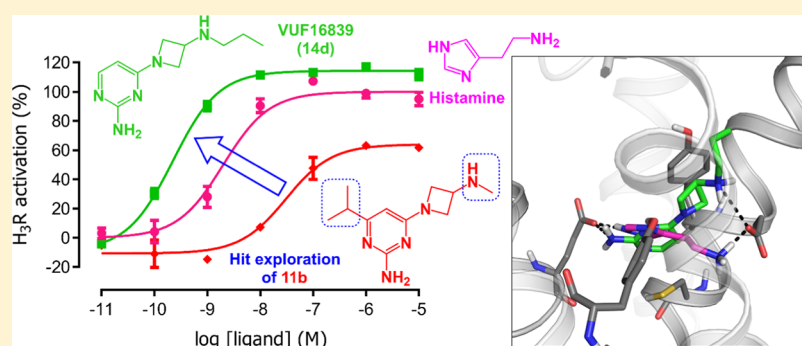
ABSTRACT: Despite the high diversity of histamine H₃ receptor (H₃R) antagonist/inverse agonist structures, partial or full H₃R agonists have typically been imidazole derivatives. An in-house screening campaign intriguingly afforded the non-imidazole 4-(3-azetidin-1-yl)pyrimidin-2-amine **11b** as a partial H₃R agonist. Here, the design, synthesis, and structure−activity relationships of **11b** analogues are described. This series yields several non-imidazole full agonists with potencies varying with the alkyl substitution pattern on the basic amine following the in vitro evaluation of H₃R agonism using a cyclic adenosine monophosphate response element-luciferase reporter gene assay. The key compound VUF16839 (**14d**) combines nanomolar on-target activity (pK_i = 8.5, pEC_{50} = 9.5) with weak activity on cytochrome P450 enzymes and good metabolic stability. The proposed H₃R binding mode of **14d** indicates key interactions similar to those attained by histamine. In vivo evaluation of **14d** in a social recognition test in mice revealed an amnesic effect at 5 mg/kg intraperitoneally. The excellent in vitro and in vivo pharmacological profiles and the non-imidazole structure of **14d** make it a promising tool compound in H₃R research.

INTRODUCTION

The four histamine receptors (H₁R, H₂R, H₃R, H₄R) belong to class A of the G protein-coupled receptor (GPCR) family.[1] The histamine H₃ receptor (H₃R) was discovered in 1983 by Arrang et al.[2] and regulates the release of several neurotransmitters such as histamine (**1**), acetylcholine, serotonin, noradrenaline, and dopamine, as both auto- and hetero-receptor.[1] Due to its expression in the cortex, striatum, and hippocampus, H₃R regulates several physiological processes such as sleep−wake regulation, cognition, and food intake.[1,3]

During the early years of discovery of H₃R ligands, the natural ligand histamine served as an initial structure for drug design, leading to a plethora of imidazole-containing ligands. However, imidazole-containing ligands are associated with drug−drug interactions due to the propensity for cytochrome P450 (CYP) inhibition and having poor brain penetration.[4,5] Therefore, research toward therapeutically relevant H₃R antagonists focused on druglike non-imidazole structures,[6,7]
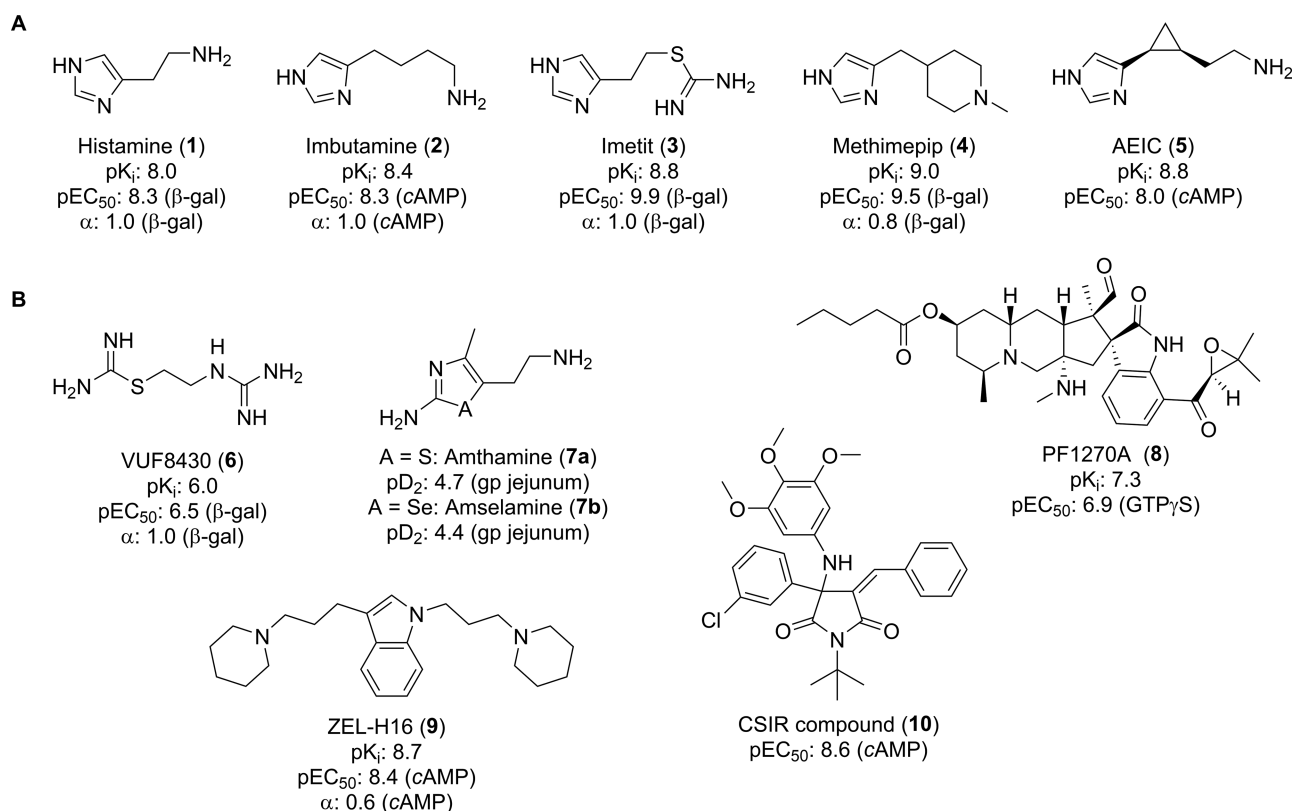
Figure 1. (A) Representative imidazole H_3R agonists. Activities are extracted from Igel et al.,[33] Govoni et al.,[18] and Kazuta et al.[12] (B) Published non-imidazole H_3R (partial) agonists.[27−32] Unless mentioned otherwise, compounds were tested on the human receptor. α, intrinsic activity compared to histamine; β-gal, cyclic adenosine monophosphate (cAMP) response element (CRE)-β-galactosidase reporter gene assay; cAMP, forskolin-stimulated cAMP accumulation assay.

and these efforts have led to numerous clinical candidates for different indications connected to central nervous system diseases, for example, Alzheimer's disease, attention deficit hyperactivity disorders, sleep disorders, schizophrenia, obesity, epilepsy, and neuropathic pain and narcolepsy.[8,9] For the latter condition, the H_3R ligand pitolisant (Wakix) was approved by the European Medicines Agency in 2016[10] and, most recently, by the Food and Drug Administration in 2019.[11]

In sharp contrast, developing non-imidazole H_3R agonists has not been very successful. The best agonists contain an imidazole ring[12−23] and, compared to the endogenous ligand histamine (**1**), these derivatives show similar [e.g., imbutamine (**2**)] or significantly higher affinity (pK_i) and/or functional activity (pEC_{50}) on H_3R [e.g., imetit (**3**), methimepip (**4**), and (1S,2S)-2-(2-aminoethyl)-1-(1H-imidazol-4-yl)cyclopropane (**5**)] (Figure 1A). Imidazole-containing agonists have shown some potential application in different therapeutic areas, such as mechanical nociception,[23] obesity, and diabetes mellitus (diet-induced obesity mice test)[24] and stress (rodent-intruder mice test).[21] Some data also support the hypothesis of cardioprotective effect of H_3R receptor activation.[25,26] However, it is fair to say that imidazole-containing agonists may suffer from the same imidazole-related drawbacks that were associated with the first generation of imidazole-containing H_3R antagonists (vide supra). Future studies on the pharmacological and therapeutic roles of H_3R agonists can therefore be helped by having non-imidazole H_3R agonists available.

A very limited number of non-imidazole agonists have been published to date (Figure 1B). VUF8430 (**6**) was designed as

an H_4R agonist based on the H_2R agonist dimaprit and shows micromolar affinity and full H_3R agonism as well.[27] The histamine analogues amthamine (**7a**) and amselamine (**7b**) were identified as H_2R agonists, but both show weak H_3R agonist activity in an electrically stimulated guinea-pig jejunum model.[28,29] Three pentacyclic spiroindolinone derivatives were isolated from *Penicillium waksmanii*, of which PF1270A (**8**) shows the best affinity for H_3R and moderate functional H_3R activity in a guanosine 5′-O-[γ-thio]triphosphate (GTPγS) accumulation assay.[30] ZEL-H16 (**9**) has been reported to have nanomolar binding affinity to the H_3R, partial H_3R agonism in forskolin-stimulated cAMP accumulation and ERK1/2 signaling assays, and full H_3R agonism in a guinea-pig ileum contraction assay.[31] Finally, a compound set with 94 examples in four compound families with either a β-lactam or a pyrrolidinone central core without basic amino moiety was published recently and surprisingly included compounds with nanomolar functional H_3R agonist activities (e.g., compound **10**).[32] The fungal isolates and the multicomponent reaction product **10** are large and complex molecules, which are difficult to align with known H_3R pharmacophores or H_3R binding modes for agonists and antagonists. We therefore started a search for novel high-affinity non-imidazole H_3R full agonists with simpler structures to generate fundamental knowledge on ligand recognition and signaling of the H_3R.

■ RESULTS

Design. During an in-house compound screen aimed at identifying agonist activities in a set of ligands using a H_3R-driven reporter gene assay in HEK293T cells, diaminopyr-
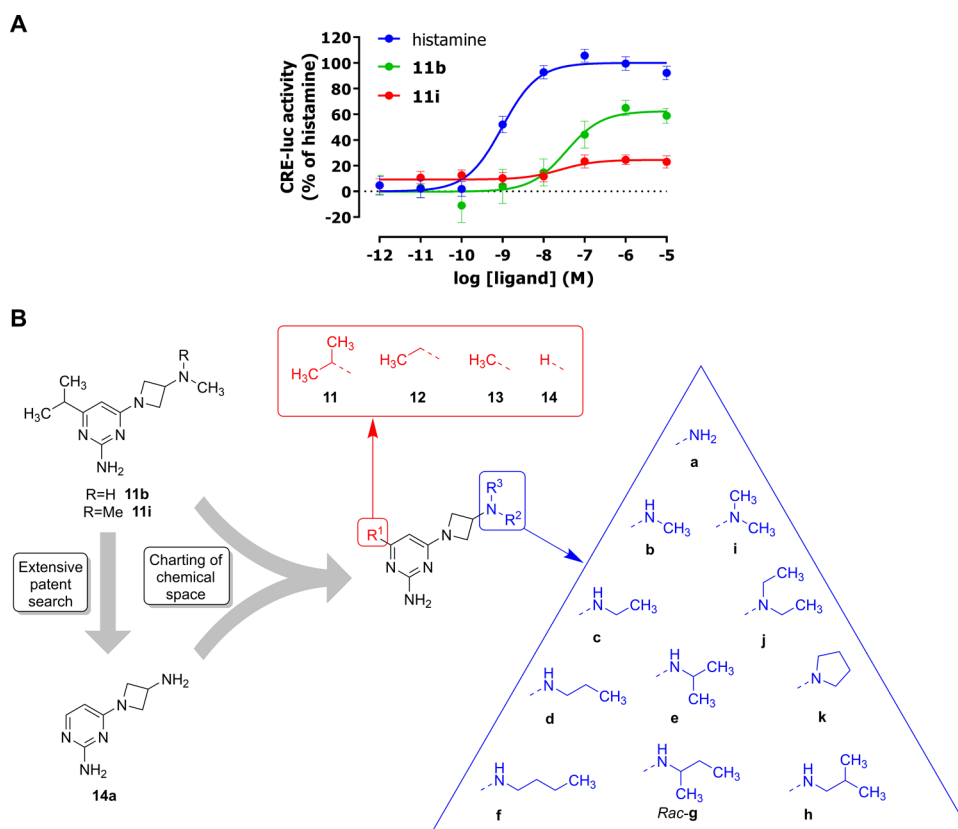
Figure 2. (A) Initial functional data of compounds **11b** and **11i** compared to histamine, as obtained by ligand-induced activation of hH$_3$R expressed on HEK293T cells measured by the CRE-luc reporter gene assay. Shown is a representative graph of at least three experiments performed in triplicate. Data are mean ± standard deviation (S.D.). (B) Structures of **11b** and **11i**, the closest relevant structure (**14a**) resulting from a subsequent extensive patent search and the compound set designed for the current study.

Scheme 1. Syntheses Routes for Final Compounds[a]
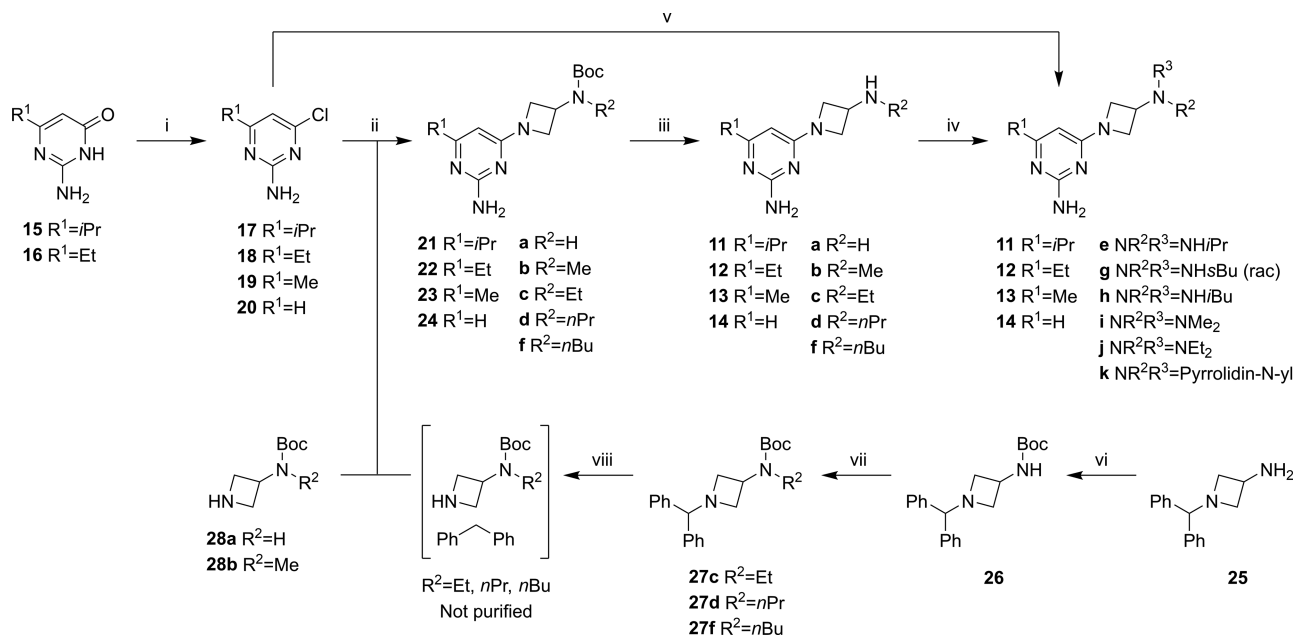
[a]Reagents and conditions: (i) POCl$_3$, 110 °C, 3 h, 26−52%; (ii) N,N-diisopropylethylamine (DIPEA), dioxane or N-methyl-2-pyrrolidone (NMP), microwave (μW), 120−150 °C, 0.5−2 h, 27−50% (**a, b**) or 35−71% (**c, d, f,** two steps from benzhydryl deprotection); (iii) HCl, dichloromethane (DCM), MeOH, room temperature (rt) to 50 °C, 3 h to overnight, 10% to quant.; (iv) aldehyde/ketone, AcOH, NaHB(OAc)$_3$, DCM, MeOH, rt, 3 h to overnight, 16−44%; or 1,4-diiodobutane, K$_2$CO$_3$, MeCN, reflux, 16 h, 9%; (v) N,N-dimethylazetidin-3-amine dihydrochloride, DIPEA, dioxane, μW, 150 °C, 30 min, 65%; (vi) di-tert-butyl dicarbonate, triethylamine (TEA), tetrahydrofuran (THF), rt, overnight, 63%; (vii) NaH, R^{2}I, THF, 0 °C to rt, overnight, 28−58%; (viii) H$_2$, Pd/C, MeOH, EtOH, rt to 60 °C, 1 h to overnight, not purified and used crude.

Table 1. Pharmacological Evaluation of Designed Compound Set
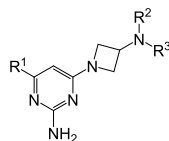
compound	R^1	R^2	R^3	$pK_i{}^c$	$pEC_{50}{}^d$	α
histamine				7.9 ± 0.2	8.6 ± 0.0	1.0 ± 0.0
11a	iPr	H	H	6.7 ± 0.0	7.1 ± 0.1	0.7 ± 0.0
11b	iPr	Me	H	7.0 ± 0.0	7.9 ± 0.4	0.7 ± 0.1
11c	iPr	Et	H	7.0 ± 0.1	6.8 ± 0.3	0.3 ± 0.1
11i	iPr	Me	Me	6.9 ± 0.0	7.0 ± 0.2	0.4 ± 0.0
12a	Et	H	H	7.1 ± 0.0	7.5 ± 0.0	0.9 ± 0.0
12b	Et	Me	H	7.3 ± 0.1	7.6 ± 0.0	0.8 ± 0.0
12c	Et	Et	H	6.9 ± 0.1	7.5 ± 0.1	0.9 ± 0.0
12i	Et	Me	Me	6.6 ± 0.2	7.2 ± 0.1	0.8 ± 0.0
13a	Me	H	H	7.3 ± 0.1	7.8 ± 0.0	0.9 ± 0.0
13b[b]	Me	Me	H	7.5 ± 0.1	8.0 ± 0.0	0.8 ± 0.1
13c	Me	Et	H	7.1 ± 0.1	7.9 ± 0.0	1.0 ± 0.0
13i	Me	Me	Me	6.5 ± 0.2	7.4 ± 0.0	0.9 ± 0.1
14a[a]	H	H	H	7.8 ± 0.1	8.3 ± 0.0	1.1 ± 0.0
14b[a]	H	Me	H	8.2 ± 0.1	8.9 ± 0.1	1.1 ± 0.1
14c[a]	H	Et	H	8.0 ± 0.1	9.2 ± 0.0	1.0 ± 0.1
14d[a]	H	nPr	H	8.5 ± 0.1	9.5 ± 0.1	1.2 ± 0.1
14e[a]	H	iPr	H	7.4 ± 0.1	8.5 ± 0.1	1.2 ± 0.1
14f[a]	H	nBu	H	7.8 ± 0.1	9.1 ± 0.3	1.2 ± 0.0
14g[a]	H	rac-sBu	H	7.9 ± 0.2	8.7 ± 0.1	1.1 ± 0.0
14h[a]	H	iBu	H	7.4 ± 0.2	8.3 ± 0.0	1.1 ± 0.0
14i[a]	H	Me	Me	7.3 ± 0.1	8.4 ± 0.1	1.0 ± 0.1
14j[a]	H	Et	Et	7.2 ± 0.1	8.1 ± 0.1	1.2 ± 0.1
14k[a]	H	-(CH₂)₄-		7.4 ± 0.1	8.1 ± 0.0	1.3 ± 0.2

[a]Measured as fumarate salt. [b]Measured as dihydrochloride salt. [c]Affinity values (pK_i) were determined by [³H]NAMH displacement assay on hH₃R expressed on HEK293T cell homogenates. [d]Potency (pEC_{50}) and intrinsic activity (α) were determined by ligand induced activation of hH₃R expressed on HEK293T cells as measured by a CRE-luciferase reporter gene assay. Data are mean ± standard error of the mean (S.E.M.) of at least three experiments performed in triplicate.

imidine **11b** emerged as a H₃R partial agonist hit ($\alpha = 0.7$), while its close derivative **11i** showed only weak agonist activity ($\alpha = 0.4$) (Figure 2A). Interestingly, a set of four diaminopyrimidine compounds has been tested before by others on H₃R en route to imbutamine (**2**) analogues, but the majority of these diaminopyrimidines were rather inactive and, where applicable, all were shown to be antagonists/inverse agonists.[34] Intrigued by the agonist activity of the diaminopyrimidine **11b** and recognizing its core as a thoroughly explored heterocycle in the H₄R area,[35] we decided to perform an in-depth patent search on this scaffold in an effort to capture the full array of industrial contributions. This resulted in the identification of **14a** (Figure 2B) as the closest derivative with data associated with H₃R (Figure 2B).[36] Remarkably, **14a** was claimed as a H₃R agonist by Abbott, although its actual synthesis was not included and only the potential synthetic route was described.[36] In the same patent, 25 related examples have been prepared, and partial agonism at the human H₃R is reported.[36]

Based on **11b** and **14a**, we designed a focused series of compounds to explore the H₃R affinity and activity in the chemical space between **14a** and **11b** (Figure 2B). The design strategy targets four series with iPr, Et, Me, or H as the R^1 group at position 6 (**11**–**14**). These R^1 groups were combined with different substituents on the basic amino groups (R^2 and R^3). Beyond the evident H (**a**) and Me (**b**) substituents,

dimethyl derivatives (**i**) were synthesized due to the potential functional switch that appears to reside in the cases of **11b** and **11i**. Based on the initial results of the designed compound set (vide infra), the R^1 = H series was extended with elongated (**d** and **f**), branched (**e**, **g**, **h**), and disubstituted (**j**, **k**) amino derivatives. This second design iteration was also inspired by previous work from our labs on the imidazole-containing agonist imbutamine (**2**), which harbors a functional switch on the basic amine.[18] Beyond **14a**, some exact compounds from this designed set are known but none in a context of H₃R. That is, **11a**, **11b**, and **12b** have been claimed as H₄R ligands,[37,38] while **12i**, **13i**, **14i**, **14j**, and **14k** were offered in chemical catalogs (April 2019) without any synthesis description and analytical or pharmacological data.

Chemistry. The designed compound set shown in Figure 2B was synthesized as outlined in Scheme 1. The key step of the synthetic route was a nucleophilic aromatic substitution on the appropriate aromatic cores with aminoazetidine moieties (step ii). The 4-chloro-2-aminopyrimidines were commercially available (**19** and **20**) or were synthesized (**17** and **18**) from the appropriate pyrimidin-4(3H)-one derivatives (**15** and **16**) with POCl₃. The R^2 = H or Me derivatives of the Boc-protected 3-aminoazetidines (**28a** and **28b**) were commercially available, while the R^2 = Et, nPr, and nBu derivatives were synthesized. These intermediates were built from benzhydryl-protected 3-aminoazetidine (**25**) with Boc protection of the
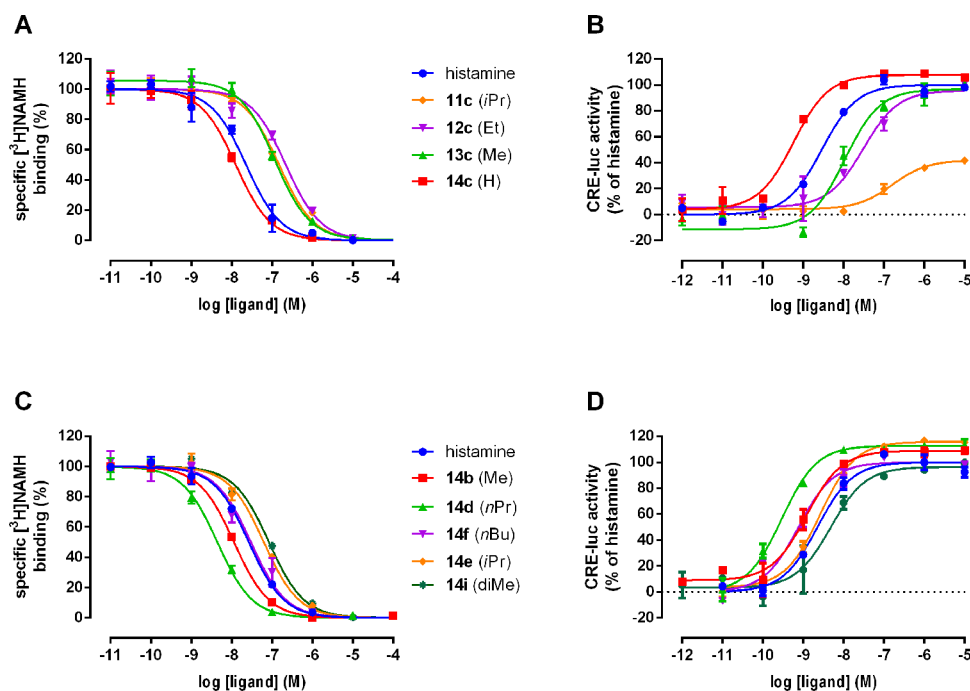
Figure 3. Representative structure−affinity relationship (A, C) and structure−function relationship (SFR) (B, D) effects selected from Table 1. (A, B) Different R^1 substituents with R^2 = Et and R^3 = H (**11c**, **12c**, **13c**, **14c**), (C, D) Different R^2 and R^3 substituents with R^1 = H (**14b**, **14d**, **14e**, **14f**, **14i**). Shown is a representative graph of at least three experiments performed in triplicate. Data are mean ± S.D.

primary amino group to give **26**, followed by alkylation with the corresponding iodoalkyl reagents resulting in the orthogonally protected intermediates (**27c**, **27d**, **27f**) and the removal of the benzhydryl group with hydrogenation. The resulting mixtures of unprotected azetidine intermediate and diphenylmethane were used directly for the ensuing nucleophilic substitution with **17**−**20**. The key nucleophilic aromatic substitution of the appropriate Boc-protected intermediates was performed in a microwave at 120−150 °C to give **21**−**24**. This was followed by the deprotection under acidic condition to afford the majority of monosubstituted (R^2 = H or linear alkyl, R^3 = H) products **11**−**14**. Although the Boc protection was necessary at the precursor stage to avoid overalkylation in the case of linear alkyl derivatives, over-alkylation was not a problem in the case of the branched-alkyl derivatives as a result of steric hindrance. Therefore, the branched-alkyl derivatives **14e**, **g**, and **h** as well as the dialkylated derivatives **12i**, **13i**, **14i**, and **14j** were synthesized from **14a** with a reductive amination. Last, **11i** was synthesized directly from **17** and *N,N*-dimethylazetidin-3-amine with a nucleophilic substitution, while the pyrrolidine ring of **14k** was obtained from 1,4-diiodobutane and **14a**.

Pharmacological Evaluation. The synthesized compound set was tested for its activity at the human H_3R transiently expressed in HEK293T cells. Binding affinity (K_i) was evaluated using a [^{3}H]NAMH displacement assay, while potency (EC_{50}) and intrinsic activity (α) were determined as the H_3R-mediated inhibition of forskolin-induced CRE-driven luciferase reporter gene activity with histamine as the control (Table 1 and Figure 3). During the first iteration, the isopropyl group of **11b** was gradually decreased in size to give **11**−**14**, which were all combined with small-size R^2/R^3 amino substituents (**a**, **b**, **c**, **i**). The affinities of the unsubstituted derivatives (**14**) stand out especially within the monomethylated (**b**) and monoethylated series (**c**), with both **14b** and **14c**

exceeding the affinity of histamine. Although monomethylated (**b**) derivatives generally show the highest affinities in each R^1 subseries **11**−**14**, the most notable variation was observed in the case of the monoethylated series **c**, with affinities of Me/Et/*i*Pr derivatives **11c**, **12c**, and **13c** being considerably reduced compared with that of **14c** (Figure 3A). A more indicative trend was observed in the case of the functional results of this **c** series. Compound **14c** has a higher potency than **14b** and produces the same intrinsic activity (α) as histamine but with higher potency (EC_{50}), while **12c** and **13c** show >1 log unit weaker EC_{50} albeit with maintained full agonism ($\alpha \sim 1.0$). Interestingly, isopropyl substitution on the R^1 position (**11c**) turns this full agonism to partial agonism (α = 0.3) (Figure 3B). A similar trend was observed in the other three series, with the pyrimidine derivatives bearing R^1 = H (**14a**−**c** and **14i**) reaching or exceeding the affinity (K_i) and potency (EC_{50}) of histamine, while any alkyl substituent at position 6 (R^1) on the pyrimidine leads to inferior results. The intrinsic activity (α) indicates full or almost full agonism ($\alpha \geq$ 0.8) in the methyl (**12a**, **12b**, **12i**) and ethyl (**13a**, **13b**, **13i**) series, while it drops to partial agonism in the isopropyl series (**11a**, **11b**, **11i**) (Table 1).

Due to the better results of the pyrimidines lacking an R^1 substituent (**14**), in a subsequent iteration the amine NHR^2 substituent was replaced with longer linear groups (**14d**, **14f**), branched groups (**14e**, **14g**, **14h**), or dialkylamino (**14j**, **14k**) moieties. Representative curves illustrate the structure−activity relationship (SAR) (Figure 3C) and SFR (Figure 3D) of this series. The *n*Pr derivative **14d** shows the highest affinity (pK_i = 8.5) from all linear monoalkyl substituents. Although both shorter and longer R^2 moieties resulted in lower binding affinities (e.g., **14c**: pK_i = 8.0 or **14f**: pK_i = 7.8), all derivatives remained in the same affinity range (Figure 3C). The branched-alkyl moieties as well as the dialkylated derivatives display loss of affinity (compare, e.g., **14d** vs **14e**, or **14b** vs
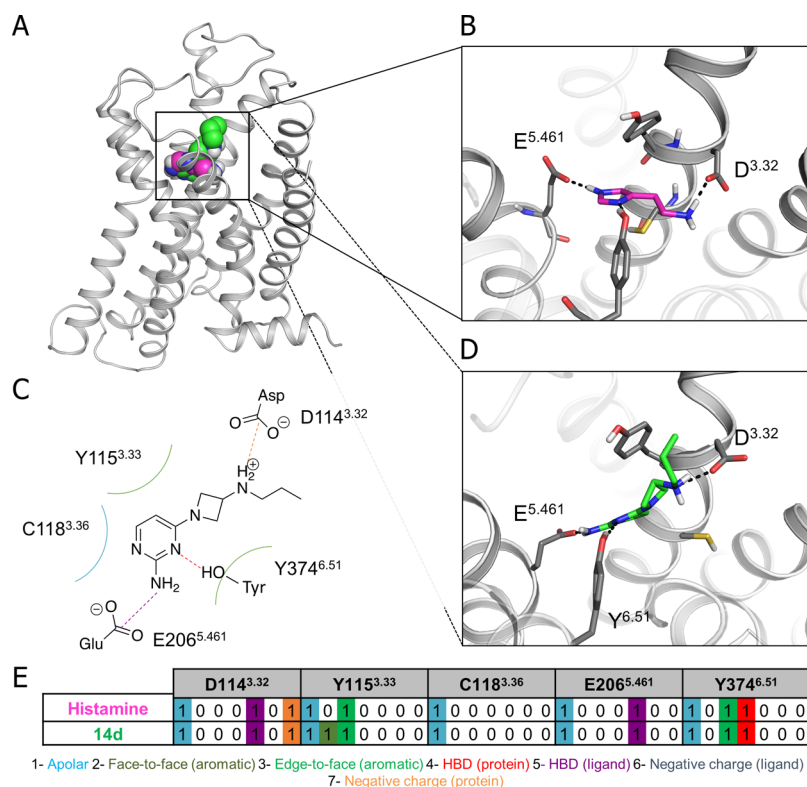
Figure 4. Predicted binding mode of **14d**. (A) Overview of the H$_3$R homology model based on the H$_1$R crystal structure (PDB ID: 3RZE).[46] The experimentally validated binding mode of histamine (magenta) is shown in more detail in (B), and the predicted binding mode of **14d** (green) is schematically represented in (C) and shown in more detail in (D). Interaction fingerprint representations of histamine and compound **14d** are shown in (E), where a one represents the presence of an interaction according to the color coding: blue for apolar, olive green for face-to-face aromatic, green for edge-to-face aromatic, red for protein hydrogen bond donor, purple for ligand hydrogen bond donor, gray for ligand-negative charge, and orange for protein-negative charge.

14i). The potencies (EC$_{50}$) show almost the same trends as observed for the affinities (Figure 3D). Highly noteworthy, the potency of **14d** (pEC$_{50}$ = 9.5) is almost a log unit higher than that of histamine (pEC$_{50}$ = 8.6), while chain shortening (e.g., **14b**, **14c**), chain lengthening (**14f**), chain branching (e.g., **14e**), or dialkylation (e.g., **14i**) results in lower potencies. In contrast to the observed differences in affinity and potency, the intrinsic activities indicate that all derivatives of **14** remain full agonists (α ≥ 1.0) (Table 1). A combination of highest affinity (pK$_i$ = 8.5), highest potency (pEC$_{50}$ = 9.5), and full agonism resides in **14d**. The potential aggregation of GPCR ligands might cause nonspecific effect on the receptor activity,[39] but nephelometry revealed no microprecipitation of **14d** up to 100 mM concentration (Figure S1) and underscores the high aqueous (aq) solubility of **14d** (soluble up to at least 100 mM in 50 mM Tris−HCl, pH 7.4). All this led to identification of **14d** as a key compound (VUF16839) in this study.

Computational Studies on 14d. A combination of molecular docking and molecular dynamics (MD) simulations was used to evaluate the potential binding mode of the key compound **14d** and to compare it to the binding mode of the endogenous ligand histamine. A homology model of H$_3$R based on the available crystal structure of H$_1$R was used (see the Experimental section). This model was validated by its ability to retrospectively discriminate between known H$_3$R fragmentlike ligands and true inactives.[40] Histamine was docked in the receptor model using PLANTS 1.1 (Figure 4A). The best-scored docking pose showing interactions with both D114$^{3.32}$ and E206$^{5.461}$ (residues known to be involved in

H$_3$R ligand binding[40−45]) was selected. During 100 ns of molecular dynamics (MD) simulations, histamine is able to maintain stable interactions with residues D114$^{3.32}$ and E206$^{5.461}$ as well as with Y374$^{6.51}$ (Figure 4B,E). Using similar procedures, compound **14d** was also docked into the same homology model using PLANTS 1.1 (Figure 4A), and the best-scored docking results show similar interactions of **14d** with D114$^{3.32}$ and E206$^{5.461}$. The basic amine of **14d** forms an ionic interaction with the negatively charged side chain of D114$^{3.32}$, and the amino group in the pyrimidine ring makes a hydrogen bond with E206$^{5.461}$. Different docking poses maintain these key interactions but show a different positioning of the linear nPr moiety at the R^2 position: toward the extracellular surface of the receptor or toward the intracellular side (Figure S2A,B, respectively). MD simulations of the two alternative models were performed (Movies 1 and 2, Supporting Information). The model in which the nPr group of **14d** is directed toward the intracellular half of the receptor was not stable along 100 ns of MD simulations (Figure S2D, Movie 2, Supporting Information), while the model where the nPr group of **14d** is pointing toward the extracellular vestibule remained stable throughout the entire simulation time (Figure S2C and Movie 1, Supporting Information). This binding mode is shown in Figure 4D, and the interactions that remained stable during the simulations are depicted in Figure 4C and the interaction fingerprints (IFPs) in Figure 4E. It can be concluded that the non-imidazole H$_3$R ligand **14d** exerts its unusual agonist H$_3$R activity by showing a similar pharmacophore as the endogenous H$_3$R ligand. That is, it may achieve its
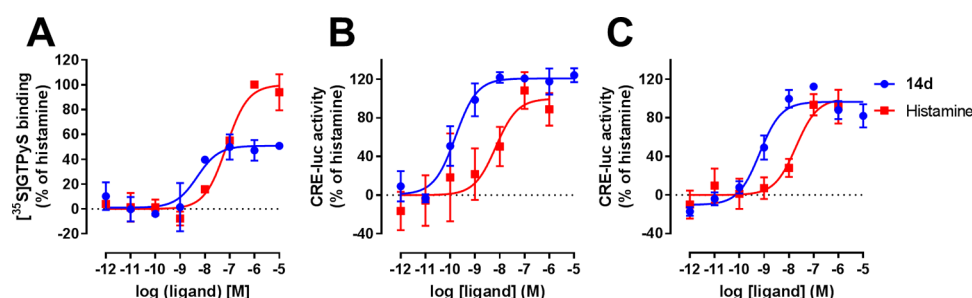
Figure 5. (A) Dose-dependent $G\alpha_i$ activation by **14d** and histamine as measured by $[^{35}S]GTP\gamma S$ accumulation on HEK293T cell homogenates expressing the hH_3R. (B, C) Dose–response curves of **14d** and histamine for ligand-induced activation of mH_3R (B) and mH_4R (C) expressed on HEK293T cells as measured by the CRE-luciferase reporter gene assay. Representative graphs of at least three experiments performed in triplicate are shown. Data are mean ± S.D.

agonist activity by forming similar interactions with the same residues as histamine.

Pharmacological and Pharmacokinetic Characterization of 14d. Functional characterization of key compound **14d** in a direct G protein activation assay, that is, the $[^{35}S]$-GTPγS accumulation assay on hH_3R expressing cell homogenates (Figure 5A), results in potent but partial agonism (pEC_{50} = 8.4 ± 0.3, α = 0.5 ± 0.05) compared with histamine (pEC_{50} = 7.2 ± 0.3, α = 1.0 ± 0.0).

Due to the high homology of the hH_3R with hH_4R (43% full sequence identity, 58% predicted transmembrane region identity),[47] several, mainly imidazole-containing, hH_3R ligands are known to possess high affinity to hH_4R as well,[33,44] although there are examples of imidazole-containing H_3R agonists with high H_3R/H_4R selectivity as well (e.g., **4** and **5**).[12,33] Therefore, **14d** was tested for its H_3R/H_4R selectivity. The pyrimidine shows only marginal selectivity with respect to binding hH_3R or hH_4R (hH_3R pK_i = 8.5 ± 0.1 vs hH_4R pK_i = 8.1 ± 0.0), but encouragingly a 10-fold selectivity in potency is observed in favor of the hH_3R (hH_3R pEC_{50} = 9.5 ± 0.1 vs hH_4R pEC_{50} = 8.5 ± 0.2) with full agonism on hH_4R (α = 1.1 ± 0.1) in a CRE-luc reporter gene assay. Moreover, **14d** does not activate the H_1R and H_2R up to 10 μM (Figure S3).

Equally encouragingly, the binding affinity of **14d** is increased for mH_3R (pK_i = 9.0 ± 0.1) compared with hH_3R, while for mH_4R, the pK_i value is decreased to 7.8 ± 0.0, thus yielding a substantial H_3R/H_4R binding selectivity for mouse receptors. Compound **14d** was also functionally evaluated as an agonist on the mH_3R and mH_4R using the CRE-luciferase reporter gene assay. In these experiments, **14d** displays a 10-fold selectivity in potency (mH_3R pEC_{50} = 10.0 ± 0.1 vs mH_4R pEC_{50} = 9.0 ± 0.1), while it acts as a full agonist on both murine receptors (mH_3R α = 1.2 ± 0.1 and mH_4R α = 1.1 ± 0.1) (Figure 5B,C).

The metabolic stability of **14d** was determined in vitro by incubation with rodent liver microsomes (Table 2). The pharmacokinetic properties for mouse [$t_{1/2}$ = 130.8 min; Cl_{int} = 20.7 mL/(min*kg)] indicate more than 2 times slower

elimination compared with the reference control verapamil.[48] For rats, this difference between **14d** and verapamil is even more pronounced.

The imidazole ring is known to generally be able to interact with CYP enzymes via coordination of the imidazole with the prosthetic heme iron, which can cause unwanted drug–drug interaction.[49] Since the 2-aminopyrimidine core contains a pattern of adjacent nitrogen atoms, we measured its propensity for CYP inhibition. Compound **14d** shows only weak activity on three key CYP enzymes (Figure S4) with IC_{50} values for binding to CYP3A4, CYP2C9, and CYP2D6 all being larger than 25 μM.

Effect of 14d on Social Recognition in Mice. Given the notion that CNS penetration of H_3R agonists,[1,5] including **14d**, is not evident, we evaluated the in vivo CNS effects of **14d** in a standard paradigm for H_3R action. It is well known that histamine, acting in different brain sites, is an important regulator of memory consolidation and retrieval in various learning paradigms, including the social recognition test.[50,51] We used this behavioral paradigm to investigate the H_3R-related CNS activity of compound **14d** in vivo. The social recognition memory investigates the ability to remember the identity of a conspecific, which is crucial to the building of social relationships and survival. Twenty-four hours after animals' habituation to the apparatus, the subject mouse was placed in an open-field arena with an empty cage and another one containing a juvenile mouse. Mice tend to spend more time in the proximity of the cage containing the juvenile mouse than the empty one, offering an indication of sociability. One hour later, the experimental mouse was placed again in the same arena, but this time one cage contained the familiar mouse and the second one a novel juvenile mouse. The exploration times of the familiar and the novel mouse were recorded separately. Compound **14d** at a dose of 5 mg/kg or vehicle was given intraperitoneally (i.p.) 30 min before the training session (Figure 6A). Compound **14d** did not affect animals' sociability as revealed by the longer time that they spent exploring the cage containing the social stimulus compared with the empty cage (Figure S5). In this respect, mice treated with compound **14d** behaved like controls. During the test session, control mice recognized the familiar juvenile, since they spent more time exploring the novel one. Conversely, mice treated with **14d** did not discriminate between the novel and the familiar mouse (Figure 6B). This result clearly suggests a social memory impairment, further confirmed by the negative discrimination index (DI) calculated for the group of animals receiving injections of **14d** (Figure 6C).

Table 2. Pharmacokinetic Properties of 14d and the Reference Drug Verapamil

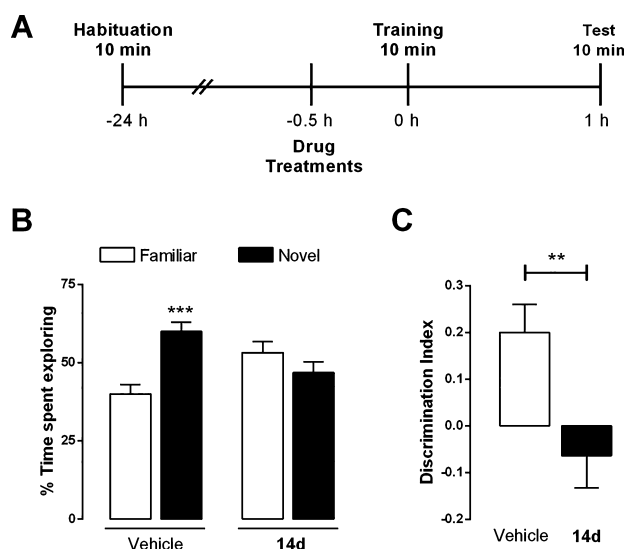|	rat liver microsomes		mouse liver microsomes	
compound	$t_{1/2}$ (min)	Cl_{int} [mL/(min*kg)]	$t_{1/2}$ (min)	Cl_{int} [mL/(min*kg)]
14d	239.0	7.9	130.8	20.7
verapamil	50.9	37.3	57.3	47.3

Figure 6. Compound **14d** impairs social recognition in mice. (A) Schematic drawings showing the sequence of procedures and treatment administrations. (B) Results are calculated as means of individual percentage of time spent exploring familiar (white columns) and novel (black columns) social stimuli. ***$P < 0.001$ vs the respective familiar subject [two-way analysis of variance (ANOVA) and Bonferroni's MCT]. (C) Discrimination index calculated according to the formula tN − tF/tN + tF. **$P < 0.01$ vs vehicle (unpaired t-test). Shown are means ± S.E.M. of 10−11 animals per experimental group.

◼ DISCUSSION AND CONCLUSIONS

We present 2-aminopyrimidine derivatives with an alkylated 3-amino-azetidine moiety showing low nanomolar affinities for the H_3R. Based on the non-imidazole partial agonist **11b** identified as an in-house hit, a 23-membered compound set was synthesized and tested on H_3R. The reduction of the substituent size at position 6 of the pyrimidine ring (R^1) improved both affinity (pK_i) and potency (pEC_{50}) on hH_3R. Each member of the extended R^1 = H series (**14**) shows full agonism in a CRE-luciferase reporter gene assay, with three derivatives (**14b−d**) improving upon the endogenous ligand histamine, combining full H_3R agonism with high (sub)-nanomolar potencies. Most notably, the key non-imidazole H_3R agonist **14d** (VUF16839) combines high affinity to the H_3R (pK_i = 8.5) with full agonism at the H_3R and a subnanomolar potency (pEC_{50} = 9.5) in a CRE-luciferase reporter gene assay. However, **14d** acts as a partial agonist in an [^{35}S]GTPγS accumulation assay with a 13-fold lower potency as compared with the more downstream CRE-luciferase reporter gene assay, which is most likely the consequence of signal amplification as suggested by a 25-fold higher potency of the full agonist histamine in the CRE-luciferase reporter gene assay as compared with an [^{35}S]GTPγS accumulation assay.

From the recent development of numerous series of H_4R antagonists, it is known that 2-aminopyrimidine is a privileged scaffold for H_4R antagonism.[35] As such, it is not surprising that **14d** also binds with relatively high affinity to the H_4R (pK_i = 8.1). It acts as an agonist at H_4R, but it is 10-fold less potent than at H_3R, while **14d** is not active at H_1R and H_2R.

The subnanomolar potency of the non-imidazole compound **14d** as an agonist at H_3R is remarkable, as so far only a few low-potency and/or complex non-imidazole ligands have been reported as agonists at H_3R.[27−32] Indeed, replacements of the imidazole ring while maintaining agonism have so far yielded little success. To illustrate, several imbutamine (**2**) analogues in which the imidazole moiety was replaced with an aminopyrimidine, aminopyridine or aminotriazole ring studied were not effective as H_3R agonists.[34] Comparing the activities of the aminopyrimidine analog of **2** with **14d**, the effective activation of H_3R by **14d** suggests a very important role of its azetidine side chain. Molecular docking combined with MD studies affords a predicted binding mode (Figure 4) in which **14d** interacts with the same key amino acids (D114$^{3.32}$, E206$^{5.461}$, Y374$^{6.51}$) as histamine (**1**) (Figure 4E), suggesting that the 2-aminopyrimidine moiety mimics the imidazole ring. The computational studies also suggest that the azetidine side chain makes an ionic interaction with the same amino acid (D114$^{3.32}$) as the amine group in the ethylamine side chain of histamine. Clearly, both **14d** and histamine are able to interact with the same key amino acids of H_3R, despite the fact that the binding modes of **14d** and histamine do not substantially overlap.

The alkyl substitution of the basic amino moiety of **2** was studied previously in our group,[18] and subtle differences in alkyl substituents on the basic amine strongly influence the functional activity of such imbutamine analogs. Based on this SAR, we hypothesize that the basic amine of the 2-aminopyrimidine compound series **11−14** might be a functional "hot spot" as well. In the case of the R^1 = iPr series (**11**), this appears to partially pan out as the chain elongation and dialkylation show moderate drops in intrinsic activity (α) (compare **11b** vs **11c** and **11i** in Table 1). However, such a trend was not observed within the other series **12−14** (Table 1 and Figure 3D).

The analysis of additional properties for key compound **14d** underscores its suitability for in vivo characterization in mice. That is, mouse potency data (mH_3R: pEC_{50} = 10.0, mH_4R: pEC_{50} = 9.0) and in vitro elimination parameters in mouse [$t_{1/2}$ = 130.8 min; Cl_{int} = 20.7 mL/(min*kg)] all bode well. The inhibition of CYP enzymes is a general issue of imidazole-containing ligands.[49] Although the diaminopyrimidine core might conceivably also be prone to CYP inhibition, **14d** only weakly (IC_{50} > 25 μM) interacts with selected key CYP enzymes (CYP3A4, CYP2D6, CYP2C9).

Poor brain penetration is a known problem of some imidazole-containing ligands,[5] limiting their potential administration routes in CNS-related experiments. As indicated by the effects in the in vivo social memory test, the 2-aminopyrimidine **14d** (5 mg/kg i.p.) is clearly penetrating the CNS. Histamine is a known modulator of different types of memory.[3,52] H_3R antagonists, such as thioperamide, improve short-term memory, while H_3R agonists such as immepip (**4**) cause amnesia in the social recognition test.[51] The results shown here confirm and expand these observations, since a memory impairment was observed also for systemic treatment with compound **14d** in the same paradigm (Figure 6). It should be noted that H_3R activation affects the circadian rhythm by increasing slow wave sleep and dose-dependently attenuates ciproxifan-induced waking effects.[53] Also, H_3R agonists reduce stress-induced behavior in preclinical models.[54] These observations suggest that H_3R activation may affect exploratory activity, which could negatively impact arousal and cognition. We did not specifically measure **14d**-induced alterations of the sleep−wake cycle; however, **14d**-associated social memory impairment does not seem to be related to

sedative effects, as there were no statistically significant differences between the control group and **14d**-treated mice in exploration time of the cage in the presence or absence of the social stimulus (during training: vehicle = 144.0 ± 60.0 s; **14d** = 136.2 ± 44.1 s; during test: vehicle = 150.5 ± 42.4 s; **14d** = 148.3 ± 69.4 s). Moreover, based on the mH$_3$R/mH$_4$R selectivity profile of **14d** (vide supra), available literature on H$_4$R expression, H$_4$R agonist actions in the CNS, and the behavioral profile of H$_4$R-deficient mice excluding a relevant role of this receptor on the histaminergic modulation of memory processing, it is highly unlikely that the in vivo amnesic effects of **14d** are confounded by its H$_4$R activity.[55,56] Indeed, the amnesic effects of **14d** are consistent with the memory impairments observed following treatment with different H$_3$R agonists [imetit (**3**) and (R)-α-methylhistamine] in the object recognition and passive avoidance tests in rats.[57]

To conclude, in this study, 2-aminopyrimidine derivatives with an alkylated 3-amino-azetidine side chain are presented as highly potent, non-imidazole agonists for the H$_3$R. The key n-propyl derivative (**14d**, VUF16839) shows attractive in vitro pharmacological properties on human H$_3$R (pK_i = 8.5, pEC$_{50}$ = 9.5, $\alpha \geq 1.0$ in a CRE-luciferase reporter gene assay with a 10-fold lower potency at H$_4$R) and mouse H$_3$R (pK_i = 9.0, pEC$_{50}$ = 10.0, with a >10-fold lower potency at mH$_4$R). It exerts reasonable metabolic stability in rodent liver microsomes and weak activity on CYP enzymes. Moreover, **14d** causes amnesic effects in social recognition tests in mice at 5 mg/kg, which is in line with the reported memory loss after administration of other H$_3$R agonists.[51,57] The observed in vivo H$_3$R effects also indicate appreciable brain penetration of **14d**. Compound **14d** can serve as a useful tool compound for fundamental studies concerning H$_3$R, given its excellent affinity and potency, H$_3$R agonism, and effective brain penetration.

■ EXPERIMENTAL SECTION

Pharmacology and ADME. *Materials.* [³H]NAMH (specific activity: 79.7 Ci/mmol) and [³H]histamine (specific activity: 17.5 Ci/mmol) were purchased from PerkinElmer (Groningen, the Netherlands). Human embryonic kidney 293T cells (HEK293T cells) were obtained from ATCC. Ketoconazole, quinidine, sulfaphenazole, and verapamil were obtained from Sigma-Aldrich (St. Louis, MO).

Cell Culture and Transfection. HEK293T cells were cultured in Dulbecco's modified Eagle's medium (DMEM) supplemented with 10% fetal bovine serum and 1% penicillin and 1% streptomycin. Two million cells per 10 cm^2 dishes were plated 24 h prior to transfection. Cells were transfected using the polyethylenimine (PEI) method.[58] For radioligand displacement assays, HEK293T cells were transfected with 2500 ng of complementary DNA (cDNA) encoding the hH$_3$R (genbank: AF140538), mH$_3$R (genbank: NM_133849.3), hH$_4$R (genbank: AY136745), or mH$_4$R (genbank: NM_153087.2) and 2500 ng of empty plasmid pcDEF3. The DNA/PEI mixture (ratio 1:4) was incubated for 20 min at 22 °C before addition to the cells.

Preparation of Cell Homogenates. Cell homogenates expressing the hH$_3$R were harvested 48 h after transfection as reported previously.[59]

Radioligand Displacement Assays. [³H]NAMH and [³H]-histamine displacement assays were performed in a binding buffer (50 mM Tris–HCl pH 7.4, 25 °C) by coincubation of 2 nM [³H]NAMH or 10 nM [³H]histamine, increasing concentrations of unlabeled ligand and cell homogenates expressing the hH$_3$R/mH$_3$R or hH$_4$R, respectively. For mH$_4$R displacement, similar studies were performed but with 30 nM [³H]histamine. The assay mixture was incubated for 2 h at 25 °C before rapid filtration over a 0.5% PEI-coated GF/C filter with a PerkinElmer filtermate harvester. The filter plate was dried, and 300 min after 25 μL of Microsint O was added,

filter-bound radioactivity was measured with a Microbeta scintillation counter (PerkinElmer).

[³⁵S]GTPγS Accumulation Assay. [³⁵S]GTPγS accumulation experiments on hH$_3$R were performed as described previously.[60]

Reporter Gene Assay. HEK293T cells were transfected in suspension with cDNA encoding hH$_3$R, mH$_3$R, hH$_4$R, mH$_4$R, H$_1$R (1000 ng) or H$_2$R (2500 ng), CRE-luciferase (2500 ng) or NFAT-luciferase (2000 ng) for H$_1$R, and empty pcDEF3 plasmid, and 50.000 cells per well were plated on a poly-L-lysine-coated white 96-well plate and grown for an additional 24 h. Cells were stimulated with increasing ligand concentrations for H$_3$R and H$_4$R in the presence of 1 μM forskolin at 37 °C and 5% CO$_2$. After 6 h, the medium was aspirated and 25 μL of luciferase assay reagent [0.83 mM adenosine 5′-triphosphate, 0.83 mM D-luciferin, 18.7 mM MgCl$_2$, 0.78 μM Na$_2$PO$_4$, 38.9 mM Tris–HCl (pH 7.8), 0.39% glycerol, 0.03% Triton-X-100, and 2.6 μM dithiothreitol] was added to each well. After 30 min of incubation at 37 °C, luminescence was measured with a Mithras plate reader (Berthold, Germany).

Data Analysis. Data were analyzed using GraphPad prism 7.02 (GraphPad Software Inc., San Diego). Shown data are mean ± S.E.M. of three individual experiments performed in triplicate unless stated otherwise. Competition binding curves were fitted to a one-site binding model. Obtained IC$_{50}$ values were converted into pK_i values using the Cheng–Prusoff equation.[61] Dose–response curves were fitted using nonlinear regression.

Metabolic Stability. The pharmacokinetic parameters of **14d** and the reference drug verapamil were estimated by using rat liver microsomes (RLMs) or mouse liver microsomes (MLMs) obtained from Sigma-Aldrich (St. Louis, MO). The tested compounds (50 μM) were incubated in the presence of microsomes (1 mg/mL) for 5, 15, 30, and 45 min in 10 mM Tris–HCl buffer (pH = 7.4) at 37 °C. Cold methanol with an internal standard (IS) was added to terminate each reaction. Next, the reaction mixtures were centrifuged at 14 500 rpm. The disappearance of the tested compounds in time was calculated by the UPLC/MS Waters ACQUITY TQD system with a TQ Detector (Waters, Milford). The course of the reaction was followed by using the analyte/IS peak height ratio values. For the determination of the $t_{1/2}$ value, the slope of linear regression from log concentration remaining versus time relationships ($-k$) was used according to Obach[48] (eq 1)

$$t_{1/2} = \frac{-0.683}{k} \tag{1}$$

Conversion of $t_{1/2}$ to intrinsic clearance Cl$_{int}$ [in units of mL/(min*kg)] was done by using eq 2

$$Cl_{int} = \frac{0.693}{t_{1/2}} \times \frac{mL\ incubation}{mg\ microsomes} \times \frac{mg\ microsomes}{g\ liver}$$
$$\times \frac{g\ liver}{kg\ b.w.} \tag{2}$$

where 45 mg of microsomal protein per gram of liver tissue (g liver) and 87 g of liver per kilogram of body weight (kg b.w.) were applied to calculate Cl$_{int}$ in mice, whereas 61 mg of microsomal protein per g liver and 45 g of liver per kg b.w. were applied to calculate Cl$_{int}$ in rats, according to Huang et al.[62] and Smith et al.[63]

Effect on CYP. Luminescent CYP3A4, CYP2D6, and CYP2C9 P450-Glo assays and protocols were obtained from Promega (Madison, WI). Compound **14d** was tested in triplicate at the final concentrations in range from 0.01 to 25 μM. The luminescent signal was measured by using a microplate reader EnSpire PerkinElmer (Waltham, MA).

Social Recognition Test. Male C57Bl6 mice (8−9 weeks old) behavior was assessed in a test apparatus comprising an open-field plexiglass arena (45 × 25 cm^2 and 20 cm high) placed in a sound-attenuated room. The assay paradigm comprises three sessions. In the first session, mice were placed in the arena containing two empty pencil-wire cups placed on opposing sides and left free to explore for 10 min. Twenty-four hours after this session, a juvenile mouse (stimulus, 4−5 weeks old), which had no prior contact with the

subject mice, was placed under one of the wire cups while the other cup remained empty. The subject mouse was then placed in the arena and was left free to explore for 10 min. During the third session, performed 1 h later, the same stimulus animal was again placed under the wire cup and a novel unfamiliar juvenile mouse was placed under the opposing cup. Subject mice were then placed again in the arena and tested for discrimination between novel and familiar mice in a 10 min session. Each mouse was subjected to the procedure separately, and care was taken to remove any olfactory/taste cues by cleaning carefully the arena and wire cups between trials. The positions of the social stimuli (empty × social; familiar × novel) were counterbalanced across subjects and trials to prevent bias from place preference. Stimulus mice were habituated to remain under the wire cups several days before behavioral testing. Vehicle or **14d** (5 mg/kg) was injected systemically (i.p.) 30 min before the second session. The animal's behavior during all sessions was videotaped, and the time spent actively exploring the stimuli was analyzed by experienced observers unaware of the experimental groups. Exploration was defined as direct snout-to-cup contact, and the time spent climbing on the cups was not considered. Data are expressed as a percentage of time spent exploring each cup (social × nonsocial during the second session or familiar × novel during the third session), and statistical significance was determined by the two-way ANOVA followed by Bonferroni's test. We also determined a sociability index, calculated according to the formula [time exploring social cup (tS) − time exploring nonsocial cup (tNS)]/[total exploration time (tS + tNS)], and a discrimination index (DI), which was calculated according to the formula [time exploring the novel mouse (tN) − time exploring the familiar mouse (tS)]/[total exploration time (tN + tF)], both analyzed using unpaired t-tests.

Computational Studies. *Residue Numbering.* Residue numbering is displayed throughout the manuscript as absolute sequence numbers and with generic numbering from GPCRdb[64] also in superscript, in which the first number denotes the helix, 1−8, and the second number denotes the residue position relative to the most-conserved residue, defined as number 50, in a gapped sequence alignment.

Homology Modeling. A three-dimensional model of the H_3R was constructed on Modeller v.9.15[65] based on the crystal structure of H_1R (PDB ID: 3RZE).[46] The sequence of H_3R was obtained from UniProt[66] and aligned to the crystal structure sequence based on the structure-based alignment of GPCRdb. An optimal structure was selected based on its ability to retrospectively discriminate between known H_3R fragmentlike ligands and true inactives as described elsewhere.[40]

Docking. A conformational library of all of the compounds was obtained with Corina v3.49[67] and protonated in ChemAxon Calculator.[68] The most energetically favorable conformations were docked using PLANTS v1.1.[69] Hundred docking poses were generated per conformation and postprocessed with interaction fingerprints (IFPs) inferred from OpenEye's OChem 1.3 library.[70,71] IFPs are bit vectors that are switched off (0) or on (1) depending on the occurrence of predefined intermolecular interactions [apolar, face-to-face, and face-to-edge aromatic interactions, hydrogen bonds (acceptor or donor), and ionic interactions (cationic or anionic)].

Molecular Dynamics Simulations and Analysis. Ligands were parametrized using the AM1-BCC charges in Antechamber.[72] The selected models were energy minimized to optimize protein−ligand interactions and used to run membrane-embedded MD simulations in GROMACS.[73] Each system was simulated for 100 ns after an equilibration of 5 ns, with the parameters and conditions described elsewhere.[74] Potential energy, root-mean-square deviation, root-mean-square fluctuation, and dihedrals of the simulations were analyzed with GROMACS tools, and residue interactions were analyzed with IFPs.

Nephelometry. In transparent flat-bottom 96-well plates, **14d** was placed at different concentrations in triplicate (10^{-1}, $10^{-1.5}$, 10^{-2}, $10^{-2.5}$, 10^{-3}, $10^{-3.5}$, 10^{-4}, and $10^{-4.5}$ M) in Tris−HCl binding buffer (50 mM Tris−HCl, pH 7.4) at least 1 h before the measurement. A Kaolin dispersion was used as a positive control[75] in each plate at different concentrations ($10^{-2.5}$, 10^{-3}, $10^{-3.5}$, 10^{-4}, $10^{-4.5}$, 10^{-5}, and $10^{-5.5}$ M) under the same conditions as with compound **14d**. Nephelometry measurements were performed with a NEPHELO star Plus (BMG Labtech, Germany) with the following settings: one cycle, measurement start time 0.1 s, measurement interval time 0.1 s, laser intensity 80%, beam focus 2.0 mm, orbital shaking mode at 200 rpm with an additional shaking time of 10 s before each cycle. Results were analyzed using Matlab R2014A (8.3.0.532) software, plotting all available data points and plotting mean and standard deviation values in a line chart compared to the Kaolin control. The linear fit (R^2) of the Kaolin control was above 0.985 in all cases.

Chemistry. *General Information.* Chemicals and solvents were obtained from commercial suppliers and were used without further purification. THF was dried by passing through the PureSolv solvent purification system by Inert. All reactions were carried out under an inert N_2 atmosphere. Hydrogenation experiments were performed with routine batch technology or the H-cube Mini Plus flow reactor. Microwave reactions were performed with the Biotage Initiator microwave system. Thin-layer chromatography analyses were performed with Merck F254 alumina silica plates using UV visualization or staining. Column purifications were carried out automatically using Biotage Isolera or Teledyne Isco CombiFlash equipment using Silicycle Ultra Pure silica gel. Melting point (mp) for final compounds was determined using a Büchi M-565 melting point apparatus at a rate of 1 °C/min. NMR spectra were recorded on a Bruker 250, 300, 500, or 600 MHz spectrometer. Chemical shifts are reported in ppm (δ), and the residual solvent was used as the internal standard (δ ^{1}H NMR: $CDCl_3$ 7.26; CD_3OD 4.87; D_2O 4.79; ^{13}C NMR: $CDCl_3$ 77.16; CD_3OD 49.00). Data are reported as follows: chemical shift, multiplicity (s, singlet; d, doublet; t, triplet; q, quartet; p, pentet; sext, sextet; hept, heptet; br, broad signal; m, multiplet; app, apparent), coupling constant(s) (Hz), and integration. High-resolution mass spectra (HRMS) were recorded on a Bruker microTOF mass spectrometer using electrospray ionization in the positive ion mode. Analytical high-performance liquid chromatography (HPLC)-mass spectrometry (MS) analyses were conducted using a Shimadzu LC-20AD liquid chromatograph pump system connected to a Shimadzu SPDM20A diode array detector with MS detection using a Shimadzu HPLC-MS 2010EV mass spectrometer. The column used is an Xbridge C18 5 mm column (50 mm × 4.6 mm). Acidic mode: solvent B (MeCN/0.1% formic acid) and solvent A (water/0.1% formic acid), flow rate of 1.0 mL/min with a run time of 8 min. For compounds whose retention time (t_R) was less than 1.5 min with the acidic solvent system, a basic solvent system was used. Basic mode: solvent B (MeCN/10% buffer), solvent A (water/10% buffer). The buffer is a 0.4% (w/v) NH_4HCO_3 solution in water, adjusted to pH 8.0 with NH_4OH. The analysis was conducted using a flow rate of 1.0 mL/min with a total run time of 8 min. Gradient settings (basic and acidic system): start 5% B, linear gradient to 90% B in 4.5 min, then isocratic for 1.5 min at 90% B, then linear gradient to 5% B in 0.5 min, then isocratic for 1.5 min at 5% B. All compounds (except **14c** and **14f**) have a purity of ≥95% calculated as the percentage peak area of the target compound by UV detection at 254 nm using the analytical HPLC-MS method listed above. Yields reported are not optimized. The compounds described in Table 1 were checked for the presence of pan assay interference compounds (PAINS) substructures as described by Baell and Holloway,[76] and no PAINS substructures were identified.

4-(3-Aminoazetidin-1-yl)-6-isopropylpyrimidin-2-amine (11a). To a solution of carbamate **21a** (351 mg, 1.14 mmol) in MeOH (20 mL) was added aq HCl (37%, 0.35 mL, 4.23 mmol). The reaction mixture was stirred at rt overnight. The solvents were removed under reduced pressure. The residue was dissolved in DCM/MeOH (10:1, 10 mL). The pH was adjusted to above 10 with NH_3 solution (7 N) in MeOH. The suspension was filtered. The solvents were removed under reduced pressure. The crude product was dissolved in hot EtOH (5 mL), and after addition of EtOAc (5 mL), a precipitate formed. The formed solid was collected by filtration, washed, and dried in vacuo. Purification by flash chromatography (DCM/MeOH/TEA 100:0:0−90:9:1) gave the title compound as a white solid (53

mg, 22%). mp: 157.0–157.6 °C. ^{1}H NMR (600 MHz, CD$_3$OD) δ 5.58 (s, 1H), 4.25 (t, J = 8.1 Hz, 2H), 3.95–3.85 (m, 1H), 3.72 (dd, J = 9.0, 5.2 Hz, 2H), 2.64 (hept, J = 7.0 Hz, 1H), 1.21 (d, J = 6.9 Hz, 6H). ^{13}C NMR (151 MHz, CD$_3$OD) δ 175.4, 165.7, 164.0, 89.8, 59.9, 44.1, 36.6, 22.0. HPLC-MS (basic mode): t_R = 2.6 min, purity: >99%, $[M + H]^+$: 208. HR-MS $[M + H]^+$ calcd for C$_{10}$H$_{18}$N$_5$$^+$: 208.1557, found 208.1564.

4-Isopropyl-6-(3-(methylamino)azetidin-1-yl)pyrimidin-2-amine *(11b)*. To a solution of carbamate **21b** (96 mg, 0.30 mmol) in DCM (5 mL) was added HCl in dioxane (4 N, 1.0 mL, 4.0 mmol). The reaction mixture was stirred for 3 h at rt. The reaction mixture was diluted with satd. aq Na$_2$CO$_3$ (10 mL) and extracted with DCM (3 × 5 mL). The combined organic phases were dried over Na$_2$SO$_4$, filtered, and concentrated in vacuo. Purification by flash chromatography (DCM/MeOH/TEA 100:0:0–90:9:1) gave the title compound as a white solid (45 mg, 68%). mp: 81.8–82.4 °C. ^{1}H NMR (500 MHz, CDCl$_3$) δ 5.47 (s, 1H), 5.05 (br, 2H), 4.23–4.15 (m, 2H), 3.76–3.63 (m, 3H), 2.65 (hept, J = 6.9 Hz, 1H), 2.42 (s, 3H), 1.19 (d, J = 6.9 Hz, 6H). ^{13}C NMR (126 MHz, CDCl$_3$) δ 173.8, 164.4, 162.0, 89.1, 56.7, 50.5, 35.4, 33.3, 21.6. HPLC-MS (basic mode): t_R = 3.1 min, purity: 97.3%, $[M + H]^+$: 222. HR-MS $[M + H]^+$ calcd for C$_{11}$H$_{20}$N$_5$$^+$: 222.1713, found 222.1718.

4-(3-(Ethylamino)azetidin-1-yl)-6-isopropylpyrimidin-2-amine *(11c)*. To a solution of carbamate **21c** (79 mg, 0.24 mmol) in MeOH (4 mL) was added aq HCl (37%, 0.19 mL, 2.29 mmol). The reaction mixture was stirred at rt overnight. The solvents were removed under reduced pressure. The residue was dissolved in DCM/MeOH (4:1, 8 mL). The pH was adjusted to above 10 with NH$_3$ solution (7 N) in MeOH. The inorganic salts were filtered off and washed with DCM/MeOH (4:1, 12 mL). The filtrate was concentrated under reduced pressure. The crude product was dissolved in hot EtOH (1 mL), and after addition of EtOAc (5 mL), a precipitate formed. The formed solid was collected by filtration, washed, and dried in vacuo. The title compound was obtained as a white solid (25 mg, 45%). mp: 226.2–227.3 °C. ^{1}H NMR (600 MHz, CD$_3$OD) δ 5.97 (s, 1H), 4.63 (br, 1H), 4.57 (br, 1H), 4.46 (br, 1H), 4.37 (br, 1H), 4.35–4.27 (m, 1H), 3.13 (q, J = 7.2 Hz, 2H), 2.87 (hept, J = 6.8 Hz, 1H), 1.38 (t, J = 7.2 Hz, 3H), 1.32 (d, J = 6.9 Hz, 6H). ^{13}C NMR (151 MHz, CD$_3$OD) δ 164.2, 163.6, 157.0, 91.5, 54.8, 54.4, 48.2, 42.4, 33.3, 20.9, 11.7. HPLC-MS (basic mode): t_R = 3.2 min, purity: >99%, $[M + H]^+$: 236. HR-MS $[M + H]^+$ calcd for C$_{12}$H$_{22}$N$_5$$^+$: 236.1870, found 236.1868.

4-(3-(Dimethylamino)azetidin-1-yl)-6-isopropylpyrimidin-2-amine *(11i)*. A microwave vial charged with amine **17** (248 mg, 1.44 mmol), N,N-dimethylazetidin-3-amine dihydrochloride (250 mg, 1.44 mmol), DIPEA (0.76 mL, 4.33 mmol), and dioxane (10 mL) was heated for 30 min at 150 °C under microwave irradiation. The reaction mixture was diluted with water (20 mL) and extracted with DCM (3 × 20 mL). The combined organic phases were dried over Na$_2$SO$_4$, filtered, and concentrated in vacuo. Purification by flash chromatography (DCM/MeOH/TEA 100:0:0–90:9:1) gave the title compound as a white solid (220 mg, 65%). mp: 123.6–123.8 °C. ^{1}H NMR (500 MHz, CDCl$_3$) δ 5.49 (s, 1H), 4.87 (br, 2H), 4.04 (t, J = 7.8 Hz, 2H), 3.94–3.81 (m, 2H), 3.21 (p, J = 5.6 Hz, 1H), 2.65 (hept, J = 6.8 Hz, 1H), 2.20 (s, 6H), 1.20 (d, J = 6.8 Hz, 6H). ^{13}C NMR (126 MHz, CDCl$_3$) δ 174.0, 164.6, 162.1, 89.1, 56.2, 53.9, 41.8, 35.5, 21.7. HPLC-MS (basic mode): t_R = 3.4 min, purity: 97.8%, $[M + H]^+$: 236. HR-MS $[M + H]^+$ calcd for C$_{12}$H$_{22}$N$_5$$^+$: 236.1870, found 236.1878.

4-(3-Aminoazetidin-1-yl)-6-ethylpyrimidin-2-amine *(12a)*. To a solution of carbamate **22a** (250 mg, 0.85 mmol) in MeOH (20 mL) was added aq HCl (37%, 0.21 mL, 2.54 mmol). The reaction mixture was stirred at rt overnight. The solvents were removed under reduced pressure. The residue was dissolved in DCM/MeOH (10:1, 40 mL). The pH was adjusted to above 10 with NH$_3$ solution (7 N) in MeOH. The suspension was filtered. The solvents were removed under reduced pressure. The crude product was dissolved in hot EtOH (5 mL), and after addition of EtOAc (15 mL), a precipitate formed. The formed solid was collected by filtration, washed, and dried in vacuo. Dissolving in H$_2$O (5 mL) and freeze-drying gave the title compound as a white fluffy solid (95 mg, 58%). mp: 224.7–225.9 °C. ^{1}H NMR

(600 MHz, CD$_3$OD) δ 5.83 (s, 1H), 4.51–4.37 (m, 2H), 4.16–4.02 (m, 3H), 2.50 (q, J = 7.6 Hz, 2H), 1.18 (t, J = 7.6 Hz, 3H). ^{13}C NMR (151 MHz, CD$_3$OD) δ 164.1, 160.2, 157.4, 92.7, 56.5, 42.6, 27.1, 12.2. HPLC-MS (basic mode): t_R = 2.3 min, purity: >99%, $[M + H]^+$: 194. HR-MS $[M + H]^+$ calcd for C$_9$H$_{16}$N$_5$$^+$: 194.1400, found 194.1410.

4-Ethyl-6-(3-(methylamino)azetidin-1-yl)pyrimidin-2-amine *(12b)*. To a solution of carbamate **22b** (450 mg, 1.46 mmol) in MeOH (20 mL) was added aq HCl (37%, 0.36 mL, 4.35 mmol). The reaction mixture was stirred at rt overnight. The solvents were removed under reduced pressure. The residue was dissolved in DCM/MeOH (10:1, 20 mL). The pH was adjusted to above 10 with NH$_3$ solution (7 N) in MeOH. The suspension was filtered. The solvents were removed under reduced pressure. The crude product was dissolved in hot EtOH (5 mL), and after addition of EtOAc (15 mL), a precipitate formed. The formed solid was collected by filtration, washed, and dried in vacuo. Dissolving in H$_2$O (5 mL) and freeze-drying gave the title compound as a white fluffy solid (150 mg, 50%). mp: 202.8–203.3 °C. ^{1}H NMR (600 MHz, CD$_3$OD) δ 5.89 (s, 1H), 4.51–4.39 (m, 2H), 4.11 (dd, J = 10.1, 3.5 Hz, 2H), 3.96 (br, 1H), 2.58 (q, J = 7.9 Hz, 2H), 2.55 (s, 3H), 1.27 (t, J = 7.6 Hz, 3H). ^{13}C NMR (151 MHz, CD$_3$OD) δ 164.1, 160.4, 157.6, 92.6, 55.9, 50.4, 32.3, 27.2, 12.2. HPLC-MS (basic mode): t_R = 2.6 min, purity: >99%, $[M + H]^+$: 208. HR-MS $[M + H]^+$ calcd for C$_{10}$H$_{18}$N$_5$$^+$: 208.1557, found 208.1566.

4-Ethyl-6-(3-(ethylamino)azetidin-1-yl)pyrimidin-2-amine *(12c)*. To a solution of carbamate **22c** (117 mg, 0.36 mmol) in MeOH (4 mL) was added aq HCl (37%, 0.30 mL, 3.62 mmol). The reaction mixture was stirred at rt overnight. The solvents were removed under reduced pressure. The residue was dissolved in DCM/MeOH (9:1, 3 mL). The pH was adjusted to above 10 with NH$_3$ solution (7 N) in MeOH. The inorganic salts were filtered off and washed with DCM/MeOH (9:1, 8 mL). The filtrate was concentrated under reduced pressure. The crude product was dissolved in hot EtOH (1.5 mL), and after addition of EtOAc (7 mL), a precipitate formed. The formed solid was collected by filtration, washed, and dried in vacuo. The title compound was obtained as a white solid (8 mg, 10%). mp: 236.6–236.9 °C. ^{1}H NMR (600 MHz, CD$_3$OD) δ 5.99 (s, 1H), 4.60 (br, 2H), 4.48–4.26 (m, 3H), 3.13 (q, J = 7.3 Hz, 2H), 2.64 (q, J = 7.6 Hz, 2H), 1.38 (t, J = 7.2 Hz, 3H), 1.31 (t, J = 7.6 Hz, 3H). ^{13}C NMR (151 MHz, CD$_3$OD) δ 164.2, 159.8, 157.0, 92.8, 54.8, 54.4, 48.2, 42.4, 26.8, 12.0, 11.7. HPLC-MS (basic mode): t_R = 2.9 min, purity: >99%, $[M + H]^+$: 222. HR-MS $[M + H]^+$ calcd for C$_{11}$H$_{20}$N$_5$$^+$: 222.1713, found 222.1703.

4-(3-(Dimethylamino)azetidin-1-yl-6-ethyl)pyrimidin-2-amine *(12i)*. To a solution of amine **12b** (110 mg, 0.53 mmol) in MeOH (5 mL) were added formaline (37%, 47 μL, 0.64 mmol) and AcOH (30 μL, 0.53 mmol). After 10 min of stirring at rt, NaBH(OAc)$_3$ (169 mg, 0.80 mmol) was added, and the resulting mixture was stirred for 3 h at rt. The reaction mixture was quenched with 5 M aq NaOH (two drops). The solvents were removed under reduced pressure. The residue was dissolved in DCM/MeOH (4:1, 8 mL). The pH was adjusted to above 10 with NH$_3$ solution (7 N) in MeOH. The inorganic salts were filtered and washed with DCM/MeOH (4:1, 12 mL). The filtrate was concentrated under reduced pressure. The crude product was purified by flash chromatography (DCM/MeOH/TEA 100:0:0–90:9:1). The selected fractions were collected, and the solvents were removed under reduced pressure. The residue was dissolved in DCM (5 mL) and washed with satd. aq Na$_2$CO$_3$ (10 mL). The aqueous phase was extracted with DCM (2 × 5 mL). The combined organic phases were dried over Na$_2$SO$_4$, filtered, and concentrated in vacuo. The residue was dissolved in MeOH (10 mL) and washed with c-hexane (20 mL). The c-hexane layer was extracted with MeOH (2 × 5 mL). The combined MeOH layers were concentrated in vacuo to give the title compound as a white solid (34 mg, 29%). mp: 128.7–128.9 °C. ^{1}H NMR (600 MHz, CD$_3$OD) δ 5.63 (s, 1H), 4.15–4.05 (m, 2H), 3.85 (dd, J = 9.0, 5.1 Hz, 2H), 3.30–3.23 (m, 1H), 2.43 (q, J = 7.6 Hz, 2H), 2.23 (s, 6H), 1.20 (t, J = 7.6 Hz, 3H). ^{13}C NMR (151 MHz, CD$_3$OD) δ 171.6, 165.6, 164.0, 91.3, 57.4, 54.7, 41.9, 31.2, 13.4. HPLC-MS (basic mode): t_R = 2.9

min, purity: >99%, [M + H]$^+$: 222. HR-MS [M + H]$^+$ calcd for C$_{11}$H$_{20}$N$_5$$^+$: 222.1713, found 222.1705.

4-(3-Aminoazetidin-1-yl)-6-methylpyrimidin-2-amine (13a). To a solution of carbamate **23a** (723 mg, 2.59 mmol) in MeOH (25 mL) was added aq HCl (37%, 3.26 mL, 39.4 mmol). The reaction mixture was stirred at rt overnight. The solvents were removed under reduced pressure. The residue was dissolved in DCM/MeOH (10:1, 40 mL). The pH was adjusted to above 10 with NH$_3$ solution (7 N) in MeOH. The suspension was filtered. The solvents were removed under reduced pressure. The crude product was recrystallized from EtOH. The crystals were collected by filtration, washed, and dried in vacuo. Dissolving in H$_2$O (5 mL) and freeze-drying gave the title compound as a white fluffy solid (189 mg, 43%). mp: 204.7−206.5 °C. ^{1}H NMR (600 MHz, CD$_3$OD) δ 5.89 (s, 1H), 4.50−4.43 (m, 2H), 4.17−4.11 (m, 1H), 4.06 (dd, J = 10.6, 4.8 Hz, 2H), 2.28 (s, 3H). ^{13}C NMR (151 MHz, CD$_3$OD) δ 164.0, 157.8, 155.9, 94.0, 57.4, 43.0, 19.3. HPLC-MS (basic mode): t_R = 2.0 min, purity: >99%, [M + H]$^+$: 180. HR-MS [M + H]$^+$ calcd for C$_8$H$_{14}$N$_5$$^+$: 180.1244, found 180.1244.

4-Methyl-6-(3-(methylamino)azetidin-1-yl)pyrimidin-2-amine Dihydrochloride (13b). To a solution of carbamate **23b** (193 mg, 0.66 mmol) in dioxane (2 mL) was added HCl in dioxane (4 N, 2.0 mL, 8.0 mmol). The reaction mixture was stirred at rt overnight. The solvents were removed under reduced pressure. The title compound was obtained as an off-white solid (176 mg, quant.). mp: 220.1−220.5 °C. ^{1}H NMR (600 MHz, CD$_3$OD/D$_2$O) δ 6.01 (s, 1H), 4.69−4.56 (m, 2H), 4.46−4.29 (m, 3H), 2.82 (s, 3H), 2.36 (s, 3H). ^{13}C NMR (151 MHz, CD$_3$OD/D$_2$O) δ 163.4, 156.2, 154.8, 94.3, 54.1, 53.7, 49.3, 31.6, 18.8. HPLC-MS (basic mode): t_R = 2.3 min, purity: >99%, [M + H]$^+$: 194. HR-MS [M + H]$^+$ calcd for C$_9$H$_{16}$N$_5$$^+$: 194.1400, found 194.1401.

4-(3-(Ethylamino)azetidin-1-yl)-6-methylpyrimidin-2-amine (13c). To a solution of carbamate **23c** (124 mg, 0.40 mmol) in MeOH (4 mL) was added aq HCl (37%, 0.33 mL, 3.99 mmol). The reaction mixture was stirred for 3 h at rt. The solvents were removed under reduced pressure. The residue was dissolved in DCM/MeOH (9:1, 8 mL). The pH was adjusted to above 10 with NH$_3$ solution (7 N) in MeOH. The inorganic salts were filtered off and washed with DCM/MeOH (4:1, 12 mL). The filtrate was concentrated under reduced pressure. The title compound was obtained as a white solid (70 mg, 84%). mp: 218.1−219.2 °C. ^{1}H NMR (600 MHz, CD$_3$OD) δ 5.85 (s, 1H), 4.44−4.34 (m, 2H), 4.03 (dd, J = 10.6, 4.8 Hz, 2H), 3.98−3.91 (m, 1H), 2.78 (q, J = 7.2 Hz, 2H), 2.26 (s, 3H), 1.20 (t, J = 7.2 Hz, 3H). ^{13}C NMR (151 MHz, CD$_3$OD) δ 164.0, 158.2, 156.4, 93.9, 56.6, 48.9, 42.2, 19.6, 13.8. HPLC-MS (basic mode): t_R = 2.7 min, purity: 96.4%, [M + H]$^+$: 208. HR-MS [M + H]$^+$ calcd for C$_{10}$H$_{18}$N$_5$$^+$: 208.1557, found 208.1549.

4-(3-(Dimethylamino)azetidin-1-yl-6-methyl)pyrimidin-2-amine (13i). Free base 4-methyl-6-(3-(methylamino)azetidin-1-yl)pyrimidin-2-amine (160 mg, 0.83 mmol) was obtained from **13b** by neutralization with NH$_3$ solution (7 N) in MeOH and filtration of the inorganic salt, followed by evaporation of the solvent. The residue was dissolved in MeOH (5 mL). To this were added formaline (37%, 74 μL, 0.99 mmol) and AcOH (47 μL, 0.83 mmol). After 10 min of stirring at rt, NaBH(OAc)$_3$ (263 mg, 1.24 mmol) was added, and the resulting mixture was stirred for 3 h at rt. The reaction mixture was quenched with 5 M aq NaOH (two drops). The solvents were removed under reduced pressure. The residue was dissolved in DCM/MeOH (4:1, 8 mL). The pH was adjusted to above 10 with NH$_3$ solution (7 N) in MeOH. The inorganic salts were filtered off and washed with DCM/MeOH (4:1, 12 mL). The filtrate was concentrated under reduced pressure. The crude product was purified by flash chromatography (DCM/MeOH/TEA 100:0:0−90:9:1). The selected fractions were collected, and the solvents were removed under reduced pressure. The residue was dissolved in DCM (5 mL) and washed with satd. aq Na$_2$CO$_3$ (10 mL). The aqueous phase was extracted with DCM (2 × 5 mL). The combined organic phases were dried over Na$_2$SO$_4$, filtered, and concentrated in vacuo. The residue was dissolved in MeOH (10 mL) and washed with *c*-hexane (20 mL). The *c*-hexane layer was extracted with MeOH (2 × 5 mL). The combined MeOH layers were concentrated in vacuo to give the title

compound as a white solid (65 mg, 38%). mp: 171.5−172.7 °C. ^{1}H NMR (600 MHz, CD$_3$OD) δ 5.63 (app d, J = 3.2 Hz, 1H), 4.15−4.04 (m, 2H), 3.91−3.80 (m, 2H), 3.30−3.23 (m, 1H), 2.23 (d, J = 2.5 Hz, 6H), 2.16 (s, 3H). ^{13}C NMR (151 MHz, CD$_3$OD) δ 166.2, 165.5, 163.9, 92.6, 57.4, 54.7, 41.9, 23.3. HPLC-MS (basic mode): t_R = 2.6 min, purity: >99%, [M + H]$^+$: 208. HR-MS [M + H]$^+$ calcd for C$_{10}$H$_{18}$N$_5$$^+$: 208.1557, found 208.1550.

4-(3-Aminoazetidin-1-yl)pyrimidin-2-amine Fumarate (14a). To a solution of carbamate **24a** (433 mg, 1.63 mmol) in MeOH (25 mL) was added aq HCl (37%, 0.74 mL, 8.94 mmol). The reaction mixture was stirred at rt overnight. The solvents were removed under reduced pressure. The residue was dissolved in DCM/MeOH (4:1, 25 mL). The pH was adjusted to above 10 with NH$_3$ solution (7 N) in MeOH. The suspension was filtered. The solvents were removed under reduced pressure. The free base (248 mg, 1.50 mmol) was dissolved in MeOH (4 mL), and fumaric acid (88 mg, 0.75 mmol) in MeOH (1 mL) was added. The clear solution was concentrated until a suspension formed. The suspension was cooled overnight at 5 °C. The formed solid was collected by filtration, washed, and dried in vacuo. Dissolving in H$_2$O (5 mL) and freeze-drying gave the title compound as a white fluffy solid (134 mg, 37%). The base-to-fumaric-acid ratio was 1:0.5 based on the ^{1}H NMR peak integration. mp: 222.7−224.1 °C. ^{1}H NMR (600 MHz, CD$_3$OD/D$_2$O) δ 7.62 (d, J = 7.3 Hz, 1H), 6.45 (s, 1H), 6.01 (d, J = 7.3 Hz, 1H), 4.57 (br, 2H), 4.38−4.15 (m, 3H). ^{13}C NMR (151 MHz, CD$_3$OD/D$_2$O) δ 174.7, 162.9, 155.8, 142.4, 136.3, 95.8, 55.4, 54.9, 41.7. HPLC-MS (basic mode): t_R = 1.7 min, purity: 96.1%, [M + H]$^+$: 166. HR-MS [M + H]$^+$ calcd for C$_7$H$_{12}$N$_5$$^+$: 166.1087, found 166.1082.

4-(3-(Methylamino)azetidin-1-yl)pyrimidin-2-amine Fumarate (14b). To a solution of carbamate **24b** (501 mg, 1.79 mmol) in MeOH (8 mL) was added aq HCl (37%, 0.54 mL, 6.52 mmol). The reaction mixture was stirred at rt overnight. The solvents were removed under reduced pressure. The residue was dissolved in DCM/MeOH (9:1, 25 mL). The pH was adjusted to above 10 with NH$_3$ solution (7 N) in MeOH. The suspension was filtered. The solvents were removed under reduced pressure. The crude free base (205 mg, 1.13 mmol) was dissolved in MeOH (25 mL), and fumaric acid (131 mg, 1.13 mmol) in MeOH (10 mL) was added. The clear solution was concentrated until a suspension formed. The suspension was cooled for 1 h at 5 °C. The formed solid was collected by filtration, washed, and dried in vacuo. Dissolving in H$_2$O (5 mL) and freeze-drying gave the title compound as a white fluffy solid (250 mg, 53%). The base-to-fumaric-acid ratio was 1:0.7 based on the ^{1}H NMR peak integration. mp: 230.1−230.5 °C. ^{1}H NMR (600 MHz, CD$_3$OD/D$_2$O) δ 7.64 (d, J = 7.0 Hz, 1H), 6.43 (s, 1H), 5.96 (d, J = 7.1 Hz, 1H), 4.46 (dd, J = 11.1, 7.6 Hz, 2H), 4.18 (dd, J = 11.2, 4.5 Hz, 2H), 4.13−4.06 (m, 1H), 2.62 (s, 3H). ^{13}C NMR (151 MHz, CD$_3$OD/D$_2$O) δ 175.2, 163.3, 157.7, 146.0, 136.5, 95.5, 54.5, 49.5, 31.8. HPLC-MS (basic mode): t_R = 2.1 min, purity: 95.6%, [M + H]$^+$: 180. HR-MS [M + H]$^+$ calcd for C$_8$H$_{14}$N$_5$$^+$: 180.1244, found 180.1238.

4-(3-(Ethylamino)azetidin-1-yl)pyrimidin-2-amine Fumarate (14c). To a solution of carbamate **24c** (117 mg, 0.40 mmol) in MeOH (4 mL) was added aq HCl (37%, 0.30 mL, 3.62 mmol). The reaction mixture was stirred at rt overnight. The solvents were removed under reduced pressure. The residue was dissolved in DCM/MeOH (9:1, 4 mL). The pH was adjusted to above 10 with NH$_3$ solution (7 N) in MeOH. The suspension was filtered. The solvents were removed under reduced pressure. The crude free base (54 mg, 0.28 mmol) was dissolved in MeOH (8 mL), and fumaric acid (32 mg, 0.28 mmol) in MeOH (3 mL) was added. After partial evaporation of MeOH and addition of EtOAc (3 mL), a precipitate was formed. The suspension was cooled for 3 h at 5 °C. The formed solid was collected by filtration, washed, and dried in vacuo. Dissolving in H$_2$O (5 mL) and freeze-drying gave the title compound as a white fluffy solid (18 mg, 17%). The base-to-fumaric-acid ratio was 1:0.6 based on the ^{1}H NMR peak integration. mp: 206.8−208.5 °C. ^{1}H NMR (600 MHz, CD$_3$OD/D$_2$O) δ 7.76 (d, J = 7.3 Hz, 1H), 6.70 (s, 1H), 6.16 (d, J = 7.3 Hz, 1H), 4.68 (br, 2H), 4.55−4.31 (m, 3H), 3.19 (q, J = 7.3 Hz, 2H), 1.41 (t, J = 7.3 Hz, 3H). ^{13}C NMR (151 MHz, CD$_3$OD/D$_2$O) δ 171.9, 163.2, 156.0, 142.7, 136.0, 95.7,

54.5, 54.1, 47.7, 42.3, 11.6. HPLC-MS (basic mode): t_R = 2.2 min, purity: 91.8%, [M + H]$^+$: 194. HR-MS [M + H]$^+$ calcd for $C_9H_{16}N_5^+$: 194.1400, found 194.1393.

4-(3-(Propylamino)azetidin-1-yl)pyrimidin-2-amine Fumarate Hydrate (14d, VUF16839). To a solution of carbamate **24d** (1.19 g, 3.87 mmol) in MeOH (20 mL) was added aq HCl (37%, 3.2 mL, 38.6 mmol). The reaction mixture was stirred at rt overnight and subsequently at 50 °C for 30 min. The solvents were removed under reduced pressure. The residue was dissolved in DCM/MeOH (4:1, 20 mL). The pH was adjusted to above 10 with NH$_3$ solution (7 N) in MeOH. The suspension was filtered. The solvents were removed under reduced pressure. The crude free base (871 mg, 3.87 mmol) was dissolved in MeOH (10 mL), and fumaric acid (453 mg, 3.90 mmol) in MeOH (10 mL) was added. The solvent was removed under reduced pressure, and the residue was recrystallized from EtOH. The suspension was cooled for 1 h at 5 °C. The crystals were filtered, washed with EtOH, and dried in vacuo. Dissolving in H$_2$O (20 mL) and freeze-drying gave the title compound as a white fluffy solid (803 mg, 58%). The base-to-fumaric-acid ratio was 1:1 based on the ^{1}H NMR peak integration. mp: 213.8–214.2 °C. ^{1}H NMR (500 MHz, D$_2$O) δ 7.61 (d, J = 7.3 Hz, 1H), 6.43 (s, 2H), 5.99 (d, J = 7.3 Hz, 1H), 4.56 (br, 2H), 4.40–4.19 (m, 3H), 3.06–2.92 (m, 2H), 1.68 (sext, J = 7.5 Hz, 2H), 0.94 (t, J = 7.4 Hz, 3H). ^{13}C NMR (151 MHz, CD$_3$OD/D$_2$O) δ 175.2, 162.9, 155.8, 142.7, 136.3, 95.7, 54.4 53.9, 48.4, 47.9, 20.2, 11.1. HPLC-MS (basic mode): t_R = 2.7 min, purity: 97.9%, [M + H]$^+$: 208. HR-MS [M + H]$^+$ calcd for $C_{10}H_{18}N_5^+$: 208.1557, found 208.1566. Anal. calcd for $C_{10}H_{17}N_5 \cdot C_4H_4O_4 \cdot$ 1.75H$_2$O: C, 47.38; H, 6.96; N, 19.73; O, 25.92; Cl, 0.00. Found: C, 47.07; H, 6.97; N, 19.43; O, 25.60; Cl, <0.1.

4-(3-(Isopropylamino)azetidin-1-yl)pyrimidin-2-amine Fumarate (14e). To a solution of free base **14a** (100 mg, 0.60 mmol) in DCM (4 mL) and MeOH (1 mL) were added acetone (48 µL, 0.66 mmol) and AcOH (34 µL, 0.60 mmol). After 10 min of stirring at rt, NaBH(OAc)$_3$ (201 mg, 0.90 mmol) was added, and the resulting mixture was stirred at rt overnight. The reaction mixture was quenched with 5 M aq NaOH (two drops). The solvents were removed under reduced pressure. The residue was purified by column chromatography (DCM/MeOH/TEA 100:0:0–80:18:2). The selected fractions were collected, and the solvents were removed under reduced pressure. The residue was dissolved in DCM/MeOH (9:1, 10 mL) and washed with satd. aq Na$_2$CO$_3$ solution (10 mL). The aqueous layer was extracted with DCM/MeOH (9:1, 2 × 5 mL). The combined organic phases were dried over Na$_2$SO$_4$, filtered, and concentrated in vacuo. The free base (32 mg, 0.154 mmol) was dissolved in MeOH (1 mL), and fumaric acid (18 mg, 0.154 mmol) in MeOH (1 mL) was added. After partial evaporation of MeOH and addition of EtOAc (5 mL), a precipitate was formed. The suspension was cooled for 1 h at 5 °C. The formed solid was collected by filtration, washed, and dried in vacuo. Dissolving in H$_2$O (5 mL) and freeze-drying gave the title compound as a white fluffy solid (42 mg, 22%). The base-to-fumaric-acid ratio was 1:1 based on the ^{1}H NMR peak integration. mp: 219.0–219.3 °C. ^{1}H NMR (500 MHz, CD$_3$OD/D$_2$O) δ 7.76 (d, J = 7.1 Hz, 1H), 6.68–6.55 (m, 2H), 6.14–6.03 (m, 1H), 4.67–4.56 (m, 2H), 4.43–4.29 (m, 3H), 3.51–3.39 (m, 1H), 1.43–1.34 (m, 6H). ^{13}C NMR (151 MHz, CD$_3$OD/D$_2$O) δ 174.2, 174.0, 163.4, 157.4, 157.1, 144.9, 144.5, 136.7, 95.5, 95.4, 55.3, 55.1, 50.9, 50.6, 46.2, 46.1, 20.0, 19.8 (multiple sets observed). HPLC-MS (basic mode): t_R = 2.7 min, purity: >99%, [M + H]$^+$: 208. HR-MS [M + H]$^+$ calcd for $C_{10}H_{18}N_5^+$: 208.1557, found 208.1566.

4-(3-(Butylamino)azetidin-1-yl)pyrimidin-2-amine Fumarate (14f). To a solution of carbamate **24f** (32 mg, 0.19 mmol) in MeOH (3 mL) was added aq HCl (37%, 0.158 mL, 1.19 mmol). The reaction mixture was stirred at rt overnight. The solvents were removed under reduced pressure. The residue was dissolved in DCM/MeOH (4:1, 5 mL). The pH was adjusted to above 10 with NH$_3$ solution (7 N) in MeOH. The suspension was filtered. The solvents were removed under reduced pressure. The free base (48 mg, 0.19 mmol) was dissolved in MeOH (1 mL), and fumaric acid (22 mg, 0.19 mmol) in MeOH (1 mL) was added. After partial evaporation of

MeOH and addition of EtOAc (5 mL), a precipitate formed. The suspension was cooled for 1 h at 5 °C. The formed solid was collected by filtration, washed, and dried in vacuo. The title compound was obtained as a white solid (34 mg, 58%). The base-to-fumaric-acid ratio was 1:0.75 based on the ^{1}H NMR peak integration. mp: 169.6–169.9 °C. ^{1}H NMR (600 MHz, CD$_3$OD/D$_2$O) δ 7.72–7.66 (m, 1H), 6.66 (s, 1H), 6.06 (d, J = 7.2 Hz, 1H), 4.54 (br, 2H), 4.34 (br, 2H), 4.27–4.21 (m, 1H), 3.02–2.95 (m, 2H), 1.72–1.64 (m, 2H), 1.43 (sext, J = 7.4 Hz, 2H), 0.97 (t, J = 7.4 Hz, 3H). ^{13}C NMR (151 MHz, CD$_3$OD/D$_2$O) δ 170.0, 163.6, 156.7, 143.1, 135.8, 95.5, 54.7, 48.6, 47.0, 29.6, 20.9, 13.9. HPLC-MS (basic mode): t_R = 3.1 min, purity: 94.6%, [M + H]$^+$: 222. HR-MS [M + H]$^+$ calcd for $C_{11}H_{20}N_5^+$: 222.1713, found 222.1705.

(rac)-4-(3-(sec-Butylamino)azetidin-1-yl)pyrimidin-2-amine Fumarate (14g). To a solution of free base **14a** (100 mg, 0.60 mmol) in DCM (4 mL) and MeOH (1 mL) were added butane-2-one (64 µL, 0.66 mmol) and AcOH (34 µL, 0.60 mmol). After 10 min of stirring at rt, NaBH(OAc)$_3$ (201 mg, 0.90 mmol) was added, and the resulting mixture was stirred at rt overnight. The reaction mixture was quenched with 5 M aq NaOH (two drops). The solvents were removed under reduced pressure. The residue was purified by column chromatography (DCM/MeOH/TEA 100:0:0–80:18:2). The selected fractions were collected, and the solvents were removed under reduced pressure. The residue was dissolved in DCM/MeOH (9:1, 10 mL) and washed with satd. aq Na$_2$CO$_3$ solution (10 mL). The aqueous layer was extracted with DCM/MeOH (9:1, 2 × 5 mL). The combined organic phases were dried over Na$_2$SO$_4$, filtered, and concentrated in vacuo. The free base (25 mg, 0.113 mmol) was dissolved in MeOH (1 mL), and fumaric acid (13 mg, 0.113 mmol) in MeOH (1 mL) was added. After partial evaporation of MeOH and addition of EtOAc (5 mL), a precipitate formed. The suspension was cooled for 1 h at 5 °C. The formed solid was collected by filtration, washed, and dried in vacuo. Dissolving in H$_2$O (5 mL) and freeze-drying gave the title compound as a white fluffy solid (32 mg, 16%). The base-to-fumaric-acid ratio was 1:1 based on the ^{1}H NMR peak integration. mp: 214.6–215.4 °C. ^{1}H NMR (500 MHz, CD$_3$OD/D$_2$O) δ 7.74 (d, J = 7.1 Hz, 1H), 6.64–6.53 (m, 2H), 6.12–6.05 (m, 1H), 4.62 (br, 2H), 4.47–4.30 (m, 3H), 3.28 (br, 1H), 1.90–1.80 (m, 1H), 1.69–1.57 (m, 1H), 1.38–1.30 (m, 3H), 1.05 (t, J = 7.5 Hz, 3H). ^{13}C NMR (151 MHz, CD$_3$OD/D$_2$O) δ 174.5, 174.1, 163.2, 156.9, 156.8, 144.3, 143.8, 136.7, 95.6, 95.5, 56.1, 56.0, 55.0, 46.1, 46.0, 27.4, 27.2, 16.3, 16.2, 9.8 (multiple sets observed). HPLC-MS (basic mode): t_R = 3.0 min, purity: 95.6%, [M + H]$^+$: 222. HR-MS [M + H]$^+$ calcd for $C_{11}H_{20}N_5^+$: 222.1713, found 222.1715.

4-(3-(Isobutylamino)azetidin-1-yl)pyrimidin-2-amine Fumarate (14h). To a solution of free base **14a** (100 mg, 0.60 mmol) in DCM (4 mL) and MeOH (1 mL) were added isobutyraldehyde (66 µL, 0.66 mmol) and AcOH (34 µL, 0.60 mmol). After 10 min of stirring at rt, NaBH(OAc)$_3$ (201 mg, 0.90 mmol) was added, and the resulting mixture was stirred at rt overnight. The reaction mixture was quenched with 5 M aq NaOH (two drops). The solvents were removed under reduced pressure. The residue was purified by column chromatography (DCM/MeOH/TEA 100:0:0–80:18:2). The selected fractions were collected, and the solvents were removed under reduced pressure. The residue was dissolved in DCM/MeOH (9:1, 10 mL) and washed with satd. aq Na$_2$CO$_3$ solution (10 mL). The aqueous layer was extracted with DCM/MeOH (9:1, 2 × 5 mL). The combined organic phases were dried over Na$_2$SO$_4$, filtered, and concentrated in vacuo. The free base (59 mg, 0.267 mmol) was dissolved in MeOH (1 mL), and fumaric acid (31 mg, 0.267 mmol) in MeOH (1 mL) was added. After partial evaporation of MeOH and addition of EtOAc (5 mL), a precipitate formed. The suspension was cooled for 1 h at 5 °C. The formed solid was collected by filtration, washed, and dried in vacuo. Dissolving in H$_2$O (5 mL) and freeze-drying gave the title compound as a white fluffy solid (78 mg, 38%). The base-to-fumaric-acid ratio was 1:1 based on the ^{1}H NMR peak integration. mp: 230.9–231.3 °C. ^{1}H NMR (500 MHz, CD$_3$OD/D$_2$O) δ 7.73 (d, J = 7.2 Hz, 1H), 6.59–6.55 (m, 2H), 6.09 (d, J = 7.2 Hz, 1H), 4.59 (t, J = 9.5 Hz, 2H), 4.37 (br app d, 2H), 4.30–4.23 (m, 1H), 2.88 (dd, J = 7.2, 3.6 Hz, 2H), 2.11–2.03 (m, 1H), 1.08 (d, J =

6.7 Hz, 6H). ^{13}C NMR (151 MHz, CD$_3$ODD$_2$O) δ 174.3, 174.2, 163.2, 156.7, 156.7, 143.7, 143.7, 136.6, 95.6, 95.5, 54.6, 54.0, 48.6, 27.3, 27.2, 20.3 (multiple sets observed). HPLC-MS (basic mode): t_R = 3.1 min, purity: >99%, [M + H]$^+$: 222. HR-MS [M + H]$^+$ calcd for C$_{11}$H$_{20}$N$_5^+$: 222.1713, found 222.1716.

4-(3-(Dimethylamino)azetidin-1-yl)pyrimidin-2-amine Fumarate (14i). To a solution of amine fumarate **14b** (100 mg, 0.34 mmol) in MeOH (25 mL) were added formaline (37%, 70 μL, 0.94 mmol) and AcOH (20 μL, 0.34 mmol). After 10 min of stirring at rt, NaBH(OAc)$_3$ (108 mg, 0.68 mmol) was added, and the resulting mixture was stirred at rt overnight. The reaction mixture was quenched with 5 M aq NaOH (two drops). The solvents were removed under reduced pressure. The residue was purified by column chromatography (DCM/MeOH/TEA 100:0:0−90:9:1). The selected fractions were collected, and the solvents were removed under reduced pressure. The residue was dissolved in DCM/MeOH (9:1, 20 mL). The pH was adjusted to above 10 with NH$_3$ solution (7 N) in MeOH. The suspension was filtered. The solvents were removed under reduced pressure. The crude free base (25 mg, 0.130 mmol) was dissolved in MeOH (5 mL), and fumaric acid (7.5 mg, 0.065 mmol) in MeOH (2.5 mL) was added. The solvent was evaporated until a suspension formed. The suspension was cooled overnight at 5 °C. The formed solid was collected by filtration, washed, and dried in vacuo. Dissolving in H$_2$O (5 mL) and freeze-drying gave the title compound as a white fluffy solid (31 mg, 36%). The base-to-fumaric-acid ratio was 1:0.5 based on the ^{1}H NMR peak integration. mp: 224.0−224.4 °C. ^{1}H NMR (500 MHz, CD$_3$OD/D$_2$O) δ 7.66 (d, J = 7.0 Hz, 1H), 6.50 (s, 1H), 5.98 (d, J = 7.0 Hz, 1H), 4.35−4.27 (m, 2H), 4.08 (dd, J = 10.8, 4.9 Hz, 2H), 3.62−3.53 (m, 1H), 2.36 (s, 6H). ^{13}C NMR (151 MHz, CD$_3$OD/D$_2$O) δ 175.0, 163.2, 157.8, 145.6, 136.7, 95.4, 56.4, 54.4, 41.5. HPLC-MS (basic mode): t_R = 2.4 min, purity: >99%, [M + H]$^+$: 194. HR-MS [M + H]$^+$ calcd for C$_9$H$_{16}$N$_5^+$: 194.1400, found 194.1395.

4-(3-(Diethylamino)azetidin-1-yl)pyrimidin-2-amine Fumarate (14j). To a solution of free base **14a** (100 mg, 0.60 mmol) in DCM (4 mL) and MeOH (1 mL) were added acetaldehyde (0.34 mL, 6 mmol) and AcOH (34 μL, 0.60 mmol). After 10 min of stirring at rt, NaBH(OAc)$_3$ (402 mg, 1.80 mmol) was added, and the resulting mixture was stirred at rt overnight. The reaction mixture was quenched with 5 M aq NaOH (two drops). The solvents were removed under reduced pressure. The residue was purified by column chromatography (DCM/MeOH/TEA 100:0:0−80:18:2). The selected fractions were collected, and the solvents were removed under reduced pressure. The residue was dissolved in DCM/MeOH (9:1, 10 mL) and washed with satd. aq Na$_2$CO$_3$ solution (10 mL). The aqueous layer was extracted with DCM/MeOH (9:1, 2 × 5 mL). The combined organic phases were dried over Na$_2$SO$_4$, filtered, and concentrated in vacuo. The free base (82 mg, 0.37 mmol) was dissolved in MeOH (1 mL), and fumaric acid (43 mg, 0.37 mmol) in MeOH (1 mL) was added. After partial evaporation of MeOH and addition of EtOAc (5 mL), a precipitate formed. The suspension was cooled for 1 h at 5 °C. The formed solid was collected by filtration, washed, and dried in vacuo. Dissolving in H$_2$O (5 mL) and freeze-drying gave the title compound as a white fluffy solid (90 mg, 44%). The base-to-fumaric-acid ratio was 1:1 based on the ^{1}H NMR peak integration. mp: 229.6−229.8 °C. ^{1}H NMR (600 MHz, CD$_3$OD/D$_2$O) δ 7.74 (d, J = 7.1 Hz, 1H), 6.64−6.55 (m, 2H), 6.10 (dd, J = 7.2, 4.0 Hz, 1H), 4.62−4.51 (m, 2H), 4.50−4.41 (m, 2H), 4.41−4.29 (m, 1H), 3.28−3.13 (m, 4H), 1.40−1.27 (m, 6H). ^{13}C NMR (151 MHz, CD$_3$OD/D$_2$O) δ 174.1, 173.8, 163.3, 157.0, 156.9, 144.1, 144.0, 136.6, 95.6, 95.5, 53.9, 52.7, 45.6, 45.4, 9.3, 9.2 (multiple sets observed). HPLC-MS (basic mode): t_R = 3.0 min, purity: 97.3%, [M + H]$^+$: 222. HR-MS [M + H]$^+$ calcd for C$_{11}$H$_{20}$N$_5^+$: 222.1713, found 222.1722.

4-(3-(Pyrrolidin-1-yl)azetidin-1-yl)pyrimidin-2-amine Fumarate (14k). To a solution of free base **14a** (100 mg, 0.60 mmol) in MeCN (20 mL) were added 1,4-diiodobutane (0.095 mL, 0.72 mmol) and K$_2$CO$_3$ (166 mg, 1.20 mmol). The resulting mixture was heated at reflux for 16 h. The solvent was removed under reduced pressure. The residue was purified by column chromatography

(DCM/MeOH/TEA 100:0:0−80:18:2). The selected fractions were collected, and the solvents were removed under reduced pressure. The residue was dissolved in DCM/MeOH (9:1, 10 mL) and washed with satd. aq Na$_2$CO$_3$ solution (10 mL). The aqueous layer was extracted with DCM/MeOH (9:1, 2 × 5 mL). The combined organic phases were dried over Na$_2$SO$_4$, filtered, and concentrated in vacuo. The free base (32 mg, 0.146 mmol) was dissolved in MeOH (1 mL), and fumaric acid (17 mg, 0.146 mmol) in MeOH (1 mL) was added. After partial evaporation of MeOH and addition of EtOAc (5 mL), a precipitate formed. The suspension was cooled for 1 h at 5 °C. The formed solid was collected by filtration, washed, and dried in vacuo. Dissolving in H$_2$O (5 mL) and freeze-drying gave the title compound as a white fluffy solid (20 mg, 9%). The base-to-fumaric-acid ratio was 1:1.15 based on the ^{1}H NMR peak integration. mp: 228.3−228.6 °C. ^{1}H NMR (600 MHz, CD$_3$OD/D$_2$O) δ 7.74 (d, J = 7.2 Hz, 1H), 6.58 (s, 2H), 6.12 (d, J = 7.2 Hz, 1H), 4.63 (br, 2H), 4.46 (br, 2H), 4.39−4.31 (m, 1H), 3.42 (br, 4H), 2.24−2.11 (m, 4H). ^{13}C NMR (151 MHz, CD$_3$OD/D$_2$O) δ 173.8, 163.2, 156.3, 143.2, 136.4, 95.6, 54.6, 54.1, 53.3, 24.2. HPLC-MS (basic mode): t_R = 2.8 min, purity: >99%, [M + H]$^+$: 220. HR-MS [M + H]$^+$ calcd for C$_{11}$H$_{18}$N$_5^+$: 220.1557, found 220.1563.

4-Chloro-6-isopropylpyrimidin-2-amine (17). Pyrimidin-4(3*H*)-one **15** (4.87 g, 31.8 mmol) was dissolved in POCl$_3$ (40 mL, 0.43 mol). The mixture was heated to reflux for 3 h. The solvent was removed under reduced pressure. Ice (150 g) was carefully added to the residue. The pH of the mixture was adjusted to 9−10 with aq NaOH (2.5 M). The mixture was extracted with DCM (3 × 100 mL). The combined organic phases were dried over Na$_2$SO$_4$, filtered, and concentrated in vacuo. Purification by flash chromatography (DCM/MeOH 10:0−9:1) gave the title compound as an off-white solid (1.41 g, 26%). ^{1}H NMR (500 MHz, CDCl$_3$) δ 6.53 (s, 1H), 5.33 (br, 2H), 2.77 (hept, J = 6.9 Hz, 1H), 1.22 (d, J = 6.9 Hz, 6H). HPLC-MS (acidic mode): t_R = 3.5 min, purity: 96.8%, [M + H]$^+$: 172.

4-Chloro-6-ethylpyrimidin-2-amine (18). Pyrimidin-4(3*H*)-one **16** (6.13 g, 44.1 mmol) was dissolved in POCl$_3$ (50 mL, 0.54 mol). The mixture was heated to reflux for 3 h. The solvent was removed under reduced pressure. Ice (150 g) was carefully added to the residue. The pH of the mixture was adjusted to 9−10 with aq NaOH (2.5 M). The mixture was extracted with DCM (3 × 10 mL). The combined organic phases were dried over Na$_2$SO$_4$, filtered, and concentrated in vacuo. Purification by flash chromatography (DCM/MeOH 10:0−9:1) gave the title compound as an off-white solid (3.63 g, 52%). ^{1}H (500 MHz, CDCl$_3$) δ 6.53 (s, 1H), 5.43 (br, 2H), 2.57 (q, J = 7.6 Hz, 2H), 1.23 (t, J = 7.6 Hz, 3H). HPLC-MS (acidic mode): t_R = 3.0 min, purity: >99%, [M + H]$^+$: 158.

tert-Butyl (1-(2-Amino-6-isopropylpyrimidin-4-yl)azetidin-3-yl)-carbamate (21a). A microwave vial charged with chloride **17** (400 g, 2.33 mmol), carbamate **28a** (402 mg, 2.33 mmol), DIPEA (0.41 mL, 2.33 mmol), and dioxane (10 mL) was heated for 120 min at 150 °C under microwave irradiation. The reaction mixture was diluted with water (20 mL) and extracted with DCM (3 × 20 mL). The combined organic phases were dried over Na$_2$SO$_4$, filtered, and concentrated in vacuo. Purification by flash chromatography (DCM/MeOH/TEA 100:0:0−90:9:1) gave the title compound as a colorless oil (351 mg, 49%). ^{1}H NMR (300 MHz, CDCl$_3$) δ 5.48 (s, 1H), 5.01 (br, 1H), 4.80 (br, 2H), 4.57 (br, 1H), 4.31 (t, J = 8.3 Hz, 2H), 3.89−3.74 (m, 2H), 2.65 (hept, J = 6.9 Hz, 1H), 1.45 (s, 9H), 1.19 (d, J = 6.9 Hz, 6H). HPLC-MS (acidic mode): t_R = 3.1 min, purity: >99%, [M + H]$^+$: 308.

tert-Butyl (1-(2-Amino-6-isopropylpyrimidin-4-yl)azetidin-3-yl)-(methyl)carbamate (21b). A microwave vial charged with chloride **17** (300 mg, 1.75 mmol), carbamate hydrochloride **28b** (389 mg, 1.75 mmol), DIPEA (0.61 mL, 3.50 mmol), and dioxane (10 mL) was heated for 30 min at 150 °C under microwave irradiation. The reaction mixture was diluted with water (20 mL) and extracted with DCM (3 × 15 mL). The combined organic phases were dried over Na$_2$SO$_4$, filtered, and concentrated in vacuo. Purification by flash chromatography (DCM/MeOH 10:0−9:1) gave the title compound as a yellow oil (280 mg, 50%). ^{1}H NMR (250 MHz, CDCl$_3$) δ 5.50 (s, 1H), 5.03 (br, 1H), 4.79 (br, 2H), 4.20 (t, J = 8.6 Hz, 2H), 4.07−

3.95 (m, 2H), 2.93 (s, 3H), 2.65 (hept, *J* = 6.9 Hz, 1H), 1.46 (s, 9H), 1.20 (d, *J* = 6.9 Hz, 6H). HPLC-MS (acidic mode): t_R = 3.4 min, purity: >99%, [M + H]⁺: 322.

tert-Butyl (1-(2-Amino-6-isopropylpyrimidin-4-yl)azetidin-3-yl)-(ethyl)carbamate (21c). Carbamate **27c** (1.02 g, 2.78 mmol) was dissolved in MeOH/EtOH (10:10 mL) and reacted with H₂ gas under atmospheric pressure using Pd/C (5%, 0.60 g) overnight at rt. The mixture was filtered over Celite, and the filtrate was concentrated in vacuo. The resulting yellowish oil (900 mg, a mixture of intermediate and diphenylmethane) was used in the next step without further purification. A microwave vial charged with chloride **17** (103 mg, 0.60 mmol), crude intermediate (221 mg), DIPEA (0.105 mL, 0.60 mmol), and dioxane (5 mL) was heated for 90 min at 150 °C under microwave irradiation. The reaction mixture was diluted with water (10 mL) and extracted with DCM (3 × 10 mL). The combined organic phases were dried over Na₂SO₄, filtered, and concentrated in vacuo. Purification by flash chromatography (DCM/MeOH 10:0−9:1) gave the title compound as a yellowish oil (79 mg, 35% over two steps, extrapolated). ¹H NMR (300 MHz, CDCl₃) *δ* 6.03 (br, 2H), 5.46 (s, 1H), 5.06 (br, 1H), 4.73 (br, 1H), 4.25 (t, *J* = 8.7 Hz, 2H), 4.17−4.05 (m, 2H), 3.33 (q, *J* = 7.0 Hz, 2H), 2.76 (hept, *J* = 6.9 Hz, 1H), 1.46 (s, 9H), 1.23 (d, *J* = 6.9 Hz, 6H), 1.14 (t, *J* = 7.0 Hz, 3H). HPLC-MS (acidic mode): t_R = 3.6 min, purity: >99%, [M + H]⁺: 336.

tert-Butyl (1-(2-Amino-6-ethylpyrimidin-4-yl)azetidin-3-yl)-carbamate (22a). A microwave vial charged with chloride **18** (500 mg, 3.17 mmol), carbamate **28a** (546 mg, 3.17 mmol), DIPEA (0.55 mL, 3.17 mmol), and dioxane (11 mL) was heated for 45 min at 150 °C under microwave irradiation. The reaction mixture was diluted with water (50 mL) and extracted with DCM (3 × 50 mL). The combined organic phases were dried over Na₂SO₄, filtered, and concentrated in vacuo. Purification by flash chromatography (DCM/MeOH 10:0−9:1) gave the title compound as a colorless oil (250 mg, 27%). ¹H NMR (300 MHz, CDCl₃) *δ* 5.49 (s, 1H), 4.99 (br, 1H), 4.78 (br, 2H), 4.58 (br, 1H), 4.31 (t, *J* = 8.3 Hz, 2H), 3.85−3.73 (m, 2H), 2.46 (q, *J* = 7.6 Hz, 2H), 1.45 (s, 9H), 1.20 (t, *J* = 7.6 Hz, 3H). HPLC-MS (acidic mode): t_R = 3.0 min, purity: 94.5%, [M + H]⁺: 294.

tert-Butyl (1-(2-Amino-6-ethylpyrimidin-4-yl)azetidin-3-yl)-(methyl)carbamate (22b). A microwave vial charged with chloride **18** (500 mg, 3.17 mmol), carbamate hydrochloride **28b** (707 mg, 3.17 mmol), DIPEA (1.11 mL, 6.35 mmol), and dioxane (11 mL) was heated for 45 min at 150 °C under microwave irradiation. The reaction mixture was diluted with water (15 mL) and extracted with DCM (3 × 10 mL). The combined organic phases were dried over Na₂SO₄, filtered, and concentrated in vacuo. Purification by flash chromatography (DCM/MeOH 10:0−9:1) gave the title compound as a colorless oil (450 mg, 46%). ¹H NMR (300 MHz, CDCl₃) *δ* 5.52 (s, 1H), 5.00 (br, 1H), 4.77 (br, 2H), 4.20 (t, *J* = 8.6 Hz, 2H), 4.07−3.94 (m, 2H), 2.92 (s, 3H), 2.47 (q, *J* = 7.6 Hz, 2H), 1.46 (s, 9H), 1.20 (t, *J* = 7.6 Hz, 3H). HPLC-MS (acidic mode): t_R = 3.1 min, purity: >99%, [M + H]⁺: 308.

tert-Butyl (1-(2-Amino-6-ethylpyrimidin-4-yl)azetidin-3-yl)-(ethyl)carbamate (22c). Carbamate **27c** (1.02 g, 2.78 mmol) was dissolved in MeOH/EtOH (10:10 mL) and reacted with H₂ gas under atmospheric pressure using Pd/C (5%, 0.60 g) overnight at rt. The mixture was filtered over Celite, and the filtrate was concentrated in vacuo. The resulting yellowish oil (900 mg, a mixture of intermediate and diphenylmethane) was used in the next step without further purification. A microwave vial charged with chloride **18** (95 mg, 0.60 mmol), crude intermediate (221 mg), DIPEA (0.105 mL, 0.60 mmol), and dioxane (5 mL) was heated for 90 min at 150 °C under microwave irradiation. The reaction mixture was diluted with water (10 mL) and extracted with DCM (3 × 10 mL). The combined organic phases were dried over Na₂SO₄, filtered, and concentrated in vacuo. Purification by flash chromatography (DCM/MeOH 10:0−9:1) gave the title compound as a yellowish oil (92 mg, 42% over two steps, extrapolated). ¹H NMR (300 MHz, CDCl₃) *δ* 5.54 (s, 1H), 4.83 (br, 3H), 4.24 (t, *J* = 8.5 Hz, 2H), 4.12−3.96 (m, 2H), 3.36 (q, *J* = 7.1 Hz, 2H), 2.49 (q, *J* = 7.6 Hz, 2H), 1.48 (s, 9H),

1.29−1.11 (m, 6H). HPLC-MS (acidic mode): t_R = 3.3 min, purity: >99% %, [M + H]⁺: 322.

tert-Butyl (1-(2-Amino-6-methylpyrimidin-4-yl)azetidin-3-yl)-carbamate (23a). A microwave vial charged with chloride **19** (1.00 g, 6.97 mmol), carbamate **28a** (1.20 g, 6.97 mmol), DIPEA (1.22 mL, 6.99 mmol), and dioxane (20 mL) was heated for 60 min at 150 °C under microwave irradiation. The reaction mixture was diluted with water (40 mL) and extracted with DCM (3 × 40 mL). The combined organic phases were dried over Na₂SO₄, filtered, and concentrated in vacuo. Purification by flash chromatography (DCM/MeOH 10:0−9:1) gave the title compound as a yellowish solid (726 mg, 36%). ¹H NMR (300 MHz, CDCl₃) *δ* 5.50 (s, 1H), 4.99 (br, 1H), 4.78 (br, 2H), 4.58 (br, 1H), 4.30 (t, *J* = 8.3 Hz, 2H), 3.83−3.73 (m, 2H), 2.20 (s, 3H), 1.45 (s, 9H). HPLC-MS (acidic mode): t_R = 2.7 min, purity: 95.5%, [M + H]⁺: 280.

tert-Butyl (1-(2-Amino-6-methylpyrimidin-4-yl)azetidin-3-yl)-(methyl)carbamate (23b). A microwave vial charged with chloride **19** (287 mg, 2.00 mmol), carbamate hydrochloride **28b** (445 mg, 2.00 mmol), DIPEA (0.70 mL, 4.00 mmol), and dioxane (4 mL) was heated for 60 min at 150 °C under microwave irradiation. The reaction mixture was diluted with water (15 mL) and extracted with DCM (3 × 10 mL). The combined organic phases were dried over Na₂SO₄, filtered, and concentrated in vacuo. Purification by flash chromatography (DCM/MeOH 100:0−92:8) gave the title compound as a colorless oil (501 mg, 46%). ¹H NMR (300 MHz, CDCl₃) *δ* 5.51 (s, 1H), 4.99 (br, 1H), 4.81 (br, 2H), 4.19 (t, *J* = 8.6 Hz, 2H), 4.06−3.93 (m, 2H), 2.91 (s, 3H), 2.19 (s, 3H), 1.46 (s, 9H). HPLC-MS (acidic mode): t_R = 2.9 min, purity: 95.9%, [M + H]⁺: 294.

tert-Butyl (1-(2-Amino-6-methylpyrimidin-4-yl)azetidin-3-yl)-(ethyl)carbamate (23c). Carbamate **27c** (1.02 g, 2.78 mmol) was dissolved in MeOH/EtOH (10:10 mL) and reacted with H₂ gas under atmospheric pressure using Pd/C (5%, 0.60 g) overnight at rt. The mixture was filtered over Celite, and the filtrate was concentrated in vacuo. The resulting yellowish oil (900 mg, a mixture of intermediate and diphenylmethane) was used in the next step without further purification. A microwave vial charged with chloride **19** (101 mg, 0.71 mmol), crude intermediate (260 mg), DIPEA (0.123 mL, 0.71 mmol), and dioxane (3 mL) was heated for 90 min at 150 °C under microwave irradiation. The reaction mixture was diluted with water (10 mL) and extracted with DCM (3 × 10 mL). The combined organic phases were dried over Na₂SO₄, filtered, and concentrated in vacuo. Purification by flash chromatography (DCM/MeOH 10:0−9:1) gave the title compound as a colorless oil (125 mg, 56% over two steps, extrapolated). ¹H NMR (300 MHz, CDCl₃) *δ* 5.52 (s, 1H), 4.75 (br, 3H), 4.20 (t, *J* = 8.5 Hz, 2H), 4.07−3.95 (m, 2H), 3.33 (q, *J* = 7.0 Hz, 2H), 2.20 (s, 3H), 1.46 (s, 9H), 1.15 (t, *J* = 7.0 Hz, 3H). HPLC-MS (acidic mode): t_R = 3.2 min, purity: >99% %, [M + H]⁺: 308.

tert-Butyl (1-(2-Aminopyrimidin-4-yl)azetidin-3-yl)carbamate (24a). A microwave vial charged with chloride **20** (500 mg, 3.86 mmol), carbamate **28a** (665 mg, 3.86 mmol), DIPEA (0.67 mL, 3.86 mmol), and dioxane (10 mL) was heated for 60 min at 150 °C under microwave irradiation. The reaction mixture was diluted with water (40 mL) and extracted with DCM (3 × 40 mL). The combined organic phases were dried over Na₂SO₄, filtered, and concentrated in vacuo. Purification by flash chromatography (DCM/MeOH 100:0−88:12) gave the title compound as a colorless oil (434 mg, 39%). ¹H NMR (300 MHz, CDCl₃) *δ* 7.83 (d, *J* = 5.8 Hz, 1H), 5.61 (d, *J* = 5.8 Hz, 1H), 5.10 (br, 1H), 4.82 (s, 2H), 4.58 (br, 1H), 4.31 (t, *J* = 8.4 Hz, 2H), 3.86−3.74 (m, 2H), 1.45 (s, 9H). HPLC-MS (acidic mode): t_R = 2.6 min, purity: 91.6%, [M + H]⁺: 266.

tert-Butyl (1-(2-Aminopyrimidin-4-yl)azetidin-3-yl)(methyl)-carbamate (24b). A microwave vial charged with chloride **20** (500 mg, 3.86 mmol), carbamate hydrochloride **28b** (723 mg, 3.86 mmol), DIPEA (1.35 mL, 7.72 mmol), and dioxane (10 mL) was heated for 30 min at 150 °C under microwave irradiation. The reaction mixture was diluted with water (40 mL) and extracted with DCM (3 × 40 mL). The combined organic phases were dried over Na₂SO₄, filtered, and concentrated in vacuo. Purification by flash chromatography (DCM/MeOH 100:0−88:12) gave the title compound as a colorless

oil (501 mg, 46%). ¹H NMR (300 MHz, CDCl₃) δ 7.84 (d, J = 5.9 Hz, 1H), 5.65 (d, J = 5.9 Hz, 1H), 5.21−4.59 (m, 3H), 4.22 (t, J = 8.7 Hz, 2H), 4.09−3.98 (m, 2H), 2.93 (s, 3H), 1.47 (s, 9H). HPLC-MS (acidic mode): t_R = 2.8 min, purity: >99%, [M + H]⁺: 280.

tert-Butyl (1-(2-Aminopyrimidin-4-yl)azetidin-3-yl)(ethyl)-carbamate (24c). Carbamate **27c** (1.02 g, 2.78 mmol) was dissolved in MeOH/EtOH (10:10 mL) and reacted with H₂ gas under atmospheric pressure using Pd/C (5%, 0.60 g) overnight at rt. The mixture was filtered through Celite. The Celite cake was washed with MeOH (2 × 5 mL), and the combined filtrates were concentrated in vacuo. The resulting yellowish oil (900 mg, a mixture of intermediate and diphenylmethane) was used in the next step without further purification. A microwave vial charged with chloride **20** (78 mg, 0.60 mmol), crude intermediate (221 mg), DIPEA (0.105 mL, 0.60 mmol), and dioxane (5 mL) was heated for 90 min at 150 °C under microwave irradiation. The reaction mixture was diluted with water (10 mL) and extracted with DCM (3 × 10 mL). The combined organic phases were dried over Na₂SO₄, filtered, and concentrated in vacuo. Purification by flash chromatography (DCM/MeOH 10:0−9:1) gave the title compound as a colorless oil (117 mg, 50% over two steps, extrapolated). ¹H NMR (300 MHz, CDCl₃) δ 7.84 (d, J = 5.8 Hz, 1H), 5.64 (d, J = 5.8 Hz, 1H), 4.77 (br, 3H), 4.22 (t, J = 8.5 Hz, 2H), 4.10−3.97 (m, 2H), 3.33 (q, J = 7.0 Hz, 2H), 1.45 (s, 9H), 1.15 (t, J = 7.0 Hz, 3H). HPLC-MS (acidic mode): t_R = 3.0 min, purity: 95.5%, [M + H]⁺: 294.

tert-Butyl (1-(2-Aminopyrimidin-4-yl)azetidin-3-yl)(propyl)-carbamate (24d). Carbamate **27d** (2.09 g, 5.49 mmol) in MeOH (100 mL) was passed through an H-cube fitted with a Pd/C (10%) catalyst cartridge at a flow rate of 1 mL/min at 60 °C and at 10 atm H₂ pressure. The solvent was removed in vacuo. The resulting colorless oil (2.03 g, a mixture of intermediate and diphenylmethane) was used in the next step without further purification. A microwave vial charged with chloride **20** (687 mg, 5.31 mmol), crude intermediate (2.03 g), DIPEA (0.93 mL, 5.27 mmol), and NMP (5 mL) was heated for 30 min at 120 °C under microwave irradiation. The mixture was purified by flash chromatography (DCM/MeOH/TEA 100:0:0−90:9:1). The selected fractions were collected, and the solvents were removed under reduced pressure. The residue was dissolved in DCM (50 mL) and washed with satd. aq Na₂CO₃ (80 mL). The aqueous phase was extracted with DCM (2 × 50 mL). The combined organic phases were dried over Na₂SO₄, filtered, and concentrated in vacuo. The title compound was obtained as a colorless oil (1.19 g, 71% over two steps). ¹H NMR (500 MHz, CDCl₃) δ 7.83 (d, J = 5.8 Hz, 1H), 5.64 (d, J = 5.8 Hz, 1H), 5.06−4.38 (m, 3H), 4.20 (t, J = 8.5 Hz, 2H), 4.07 (t, J = 7.6 Hz, 2H), 3.22 (t, J = 7.6 Hz, 2H), 1.54 (sext, J = 7.4 Hz, 2H), 1.44 (s, 9H), 0.88 (t, J = 7.4 Hz, 3H). HPLC-MS (acidic mode): t_R = 3.3 min, purity: >99%, [M + H]⁺: 308.

tert-Butyl (1-(2-Aminopyrimidin-4-yl)azetidin-3-yl)(butyl)-carbamate (24f). A solution of carbamate **27f** (178 mg, 0.45 mmol) in MeOH (16 mL) was passed through an H-cube fitted with a Pd/C (10%) catalyst cartridge at a flow rate of 1 mL/min at 60 °C and at 10 atm H₂ pressure. The solvent was removed in vacuo. The resulting colorless oil (136 mg, a mixture of intermediate and diphenylmethane) was used in the next step without further purification. A microwave vial charged with chloride **20** (44 mg, 0.34 mmol), crude intermediate (136 mg), DIPEA (0.060 mL, 0.34 mmol), and NMP (0.5 mL) was heated for 30 min at 120 °C under microwave irradiation. The mixture was purified by flash chromatography (DCM/MeOH/TEA 100:0:0−80:18:2). The title compound was obtained as an off-white solid (62 mg, 46% over two steps). ¹H NMR (300 MHz, CD₃OD) δ 7.71 (d, J = 6.2 Hz, 1H), 5.77 (d, J = 6.0 Hz, 1H), 4.54 (s, 1H), 4.32−4.14 (m, 4H), 3.35−3.25 (m, 2H), 1.62−1.47 (m, 2H), 1.44 (s, 9H), 1.38−1.24 (m, 2H), 0.98−0.90 (m, 3H). HPLC-MS (acidic mode): t_R = 3.4 min, purity: 97.5%, [M + H]⁺: 322.

tert-Butyl (1-Benzhydrylazetidin-3-yl)carbamate (26). To a solution of amine **25** (5.00 g, 21.0 mmol) in THF (40 mL) at 0 °C was added a solution of di-*tert*-butyl dicarbonate (5.40, 25.2 mmol) in THF (40 mL) and TEA (3.51 mL, 25.2 mmol). The reaction mixture was warmed to rt and stirred for 2 h. The solvent was evaporated. Purification by flash chromatography (*c*-hexane/EtOAc/TEA 100:0:0−0:95:5) gave the title compound as a white solid (4.45 g, 63%). ¹H NMR (300 MHz, CDCl₃) δ 7.39 (d, J = 7.6 Hz, 4H), 7.32−7.22 (m, 4H), 7.22−7.12 (m, 2H), 4.87 (br, 1H), 4.30 (br, 2H), 3.53 (t, J = 6.3 Hz, 2H), 2.82 (br, 2H), 1.42 (s, 9H). HPLC-MS (acidic mode): t_R = 3.5 min, purity: 97.5%, [M + H]⁺: 339.

tert-Butyl (1-Benzhydrylazetidin-3-yl)(ethyl)carbamate (27c). To a solution of carbamate **26** (3.10 g, 9.2 mmol) in THF (30 mL) at 0 °C, NaH (60%, 0.44 g, 11.0 mmol) was added. When the evolution of H₂ gas subsided, iodoethane (0.81 mL, 10.1 mmol) was added dropwise to the reaction mixture. The resulting mixture was stirred overnight at rt. The reaction mixture was diluted with water (60 mL) and extracted with DCM (3 × 40 mL). The combined organic phases were dried over Na₂SO₄, filtered, and concentrated in vacuo. Purification by flash chromatography (*c*-hexane/EtOAc 10:0−7:3) gave the title compound as a white solid (1.95 g, 58%). ¹H NMR (300 MHz, CDCl₃) δ 7.48−7.35 (m, 4H), 7.32−7.23 (m, 4H), 7.23−7.12 (m, 2H), 4.34 (br, 2H), 3.51 (br, 2H), 3.27 (q, J = 7.1 Hz, 2H), 2.95 (br, 2H), 1.42 (s, 9H), 1.05 (t, J = 7.0 Hz, 3H). HPLC-MS (acidic mode): t_R = 3.9 min, purity: 99.6%, [M + H]⁺: 367.

tert-Butyl (1-Benzhydrylazetidin-3-yl)(propyl)carbamate (27d). To a solution of carbamate **26** (4.55 g, 13.2 mmol) in THF (30 mL) at 0 °C, NaH (95%, 0.40 g, 10.5 mmol) was added. When the evolution of H₂ gas subsided, iodopropane (1.44 mL, 14.7 mmol) was added dropwise to the reaction mixture. The resulting mixture was stirred overnight at rt. The reaction mixture was diluted with water (200 mL) and extracted with DCM (3 × 120 mL). The combined organic phases were dried over Na₂SO₄, filtered, and concentrated in vacuo. Purification by flash chromatography (*c*-hexane/EtOAc/TEA 100:0:0−70:28.5:1.5) gave the title compound as a white solid (2.09 g, 42%). ¹H NMR (300 MHz, CDCl₃) δ 7.46−7.35 (m, 4H), 7.33−7.23 (m, 4H), 7.23−7.14 (m, 2H), 4.33 (s, 2H), 3.50 (t, J = 7.2 Hz, 2H), 3.22−3.10 (m, 2H), 2.93 (t, J = 6.9 Hz, 2H), 1.51−1.36 (m, 11H), 0.85 (t, J = 7.4 Hz, 3H). HPLC-MS (acidic mode): t_R = 3.9 min, purity: 99.3%, [M + H]⁺: 381.

tert-Butyl (1-Benzhydrylazetidin-3-yl)(butyl)carbamate (27f). To a solution of carbamate **26** (552 mg, 1.60 mmol) in THF (50 mL) at 0 °C, NaH (60%, 77 mg, 1.92 mmol) was added. When the evolution of H₂ gas subsided, iodobutane (0.20 mL, 1.76 mmol) was added dropwise to the reaction mixture. The resulting mixture was stirred overnight at rt. The reaction mixture was diluted with water (20 mL) and extracted with DCM (3 × 15 mL). The combined organic phases were dried over Na₂SO₄, filtered, and concentrated in vacuo. Purification by flash chromatography (*c*-hexane/EtOAc/TEA 100:0:0−0:95:5) gave the title compound as a white solid (178 mg, 28%). ¹H NMR (300 MHz, CDCl₃) δ 7.46−7.36 (m, 4H), 7.32−7.23 (m, 4H), 7.23−7.14 (m, 2H), 4.33 (s, 2H), 3.59−3.35 (m, 2H), 3.26−3.12 (m, 2H), 2.93 (br, 2H), 1.50−1.34 (m, 11H, overlaps with residual *c*-hexane), 1.33−1.17 (m, 2H), 0.90 (t, J = 7.2 Hz, 3H). HPLC-MS (acidic mode): t_R = 4.4 min, purity: 97.8%, [M + H]⁺: 395.

■ ASSOCIATED CONTENT

Ⓢ Supporting Information

The Supporting Information is available free of charge on the ACS Publications website at DOI: 10.1021/acs.jmed-chem.9b01462.

> Nephelometry results of **14d**; best-scored docking poses of **14d**; functional assay on H₁R and H₂R; effect of **14d** on CYP3A4, CYP2D6, and CYP2C9 activities; sociability effect of **14d** in the social recognition test in mice; HPLC-MS chromatogram and spectra of **14d** (PDF)
> Biochemical data of **1**, **11a** to **14k** (XLS)
> Molecular formula strings (CSV)
> MD simulations of the model where the *n*Pr group of **14d** is pointing toward the extracellular vestibule (Movie 1) (MPG)

MD simulations of the model where the *n*Pr group of **14d** is directed toward the intracellular half of the receptor (Movie 2) (MPG)

■ AUTHOR INFORMATION

Corresponding Author
*E-mail: r.leurs@vu.nl. Phone: +31 20 59 87579.
ORCID
Gábor Wágner: 0000-0001-5111-6749
Marta Arimont: 0000-0002-9367-5298
Henry F. Vischer: 0000-0002-0184-6337
Maikel Wijtmans: 0000-0001-8955-8016
Rob Leurs: 0000-0003-1354-2848
Notes
The authors declare no competing financial interest.

■ ABBREVIATIONS

α, intrinsic activity compared to histamine; cAMP, cyclic adenosine monophosphate; CRE, *c*AMP response element; DCM, dichloromethane; DIPEA, *N*,*N*-diisopropylethylamine; FLIPR, fluorometric imaging plate reader; GPCR, G protein-coupled receptor; GTPγS, guanosine $5'$-O-$[\gamma$-thio]-triphosphate; IFP, interaction fingerprint; i.p., intraperitoneal; mp, melting point; MD, molecular dynamics; NAMH, *N*-α-methylhistamine; NMP, *N*-methyl-2-pyrrolidone; SAR, structure−activity relationship; satd. aq, saturated aqueous; S.D., standard deviation; S.E.M., standard error of mean; SFR, structure−function relationship; rt, room temperature; TEA, triethylamine; THF, tetrahydrofuran; μW, microwave reaction

■ REFERENCES

(1) Panula, P.; Chazot, P. L.; Cowart, M.; Gutzmer, R.; Leurs, R.; Liu, W. L. S.; Stark, H.; Thurmond, R. L.; Haas, H. L. International Union of Basic and <tep-common:author-query>AQ9: Please check whether the updated information in ref 1 is correct.</tep-common:author-query>Clinical Pharmacology. XCVIII. Histamine receptors. *Pharmacol. Rev.* **2014**, *67*, 601−655.

(2) Arrang, J. M.; Garbarg, M.; Schwartz, J. C. Auto-inhibition of brain histamine release mediated by a novel class (H₃) of histamine receptor. *Nature* **1983**, *302*, 832−837.

(3) Schlicker, E.; Kathmann, M. Role of the histamine H₃ receptor in the central nervous system. *Handb. Exp. Pharmacol.* **2017**, *241*, 277−299.

(4) Stark, H.; Kathmann, M.; Schlicker, E.; Schunack, W.; Schlegel, B.; Sippl, W. Medicinal chemical and pharmacological aspects of imidazole-containing histamine H3 receptor antagonists. *Mini-Rev. Med. Chem.* **2004**, *4*, 965−977.

(5) Ganellin, C. R.; Leurquin, F.; Piripitsi, A.; Arrang, J. M.; Garbarg, M.; Ligneau, X.; Schunack, W.; Schwartz, J.-C. Synthesis of potent non-imidazole histamine H₃-receptor antagonists. *Arch. Pharm.* **1998**, *331*, 395−404.

(6) Celanire, S.; Wijtmans, M.; Talaga, P.; Leurs, R.; de Esch, I. J. P. Keynote review: Histamine H₃ receptor antagonists reach out for the clinic. *Drug Discovery Today* **2005**, *10*, 1613−1627.

(7) Lebois, E. P.; Jones, C. K.; Lindsley, C. W. The evolution of histamine H₃ antagonists/inverse agonists. *Curr. Top. Med. Chem.* **2011**, *11*, 648−660.

(8) Kuhne, S.; Wijtmans, M.; Lim, H. D.; Leurs, R.; de Esch, I. J. P. Several down, a few to go: histamine H₃ receptor ligands making the final push towards the market? *Expert Opin. Invest. Drugs* **2011**, *20*, 1629−1648.

(9) Sadek, B.; Łażewska, D.; Hagenow, S.; Kieć-Kononowicz, K.; Stark, H. Histamine H₃R Antagonists: From Scaffold Hopping to Clinical Candidates. In *Histamine Receptors*; Blandina, P., Passani, M., Eds.; The Receptors; Humana Press: Cham, 2016; Vol. 28, pp 109−155.

(10) Kollb-Sielecka, M.; Demolis, P.; Emmerich, J.; Markey, G.; Salmonson, T.; Haas, M. The European Medicines Agency review of pitolisant for treatment of narcolepsy: summary of the scientific assessment by the Committee for Medicinal Products for Human Use. *Sleep Med.* **2017**, *33*, 125−129.

(11) Harmony Biosciences LLC. https://www.harmonybiosciences.com/newsroom/harmony-biosciences-announces-fda-approval-of-wakix-r-pitolisant-a-first-in/ (accessed Aug 15, 2019).

(12) Kazuta, Y.; Hirano, K.; Natsume, K.; Yamada, S.; Kimura, R.; Matsumoto, S. I.; Furuichi, K.; Matsuda, A.; Shuto, S. Cyclopropane-based conformational restriction of histamine. (1S,2S)-2-(2-amino-ethyl)-1-(1H-imidazol-4-yl)cyclopropane, a highly selective agonist for the histamine H₃ receptor, having a cis-cyclopropane structure. *J. Med. Chem.* **2003**, *46*, 1980−1988.

(13) Kitbunnadaj, R.; Zuiderveld, O. P.; de Esch, I. J. P.; Vollinga, R. C.; Bakker, R.; Lutz, M.; Spek, A. L.; Cavoy, E.; Deltent, M.-F.; Menge, W. M. P. B.; Timmerman, H.; Leurs, R. Synthesis and structure−activity relationships of conformationally constrained histamine H₃ receptor agonists. *J. Med. Chem.* **2003**, *46*, 5445−5457.

(14) Kitbunnadaj, R.; Zuiderveld, O. P.; Christophe, B.; Hulscher, S.; Menge, W. M. P. B.; Gelens, E.; Snip, E.; Bakker, R. A.; Celanire, S.; Gillard, M.; Talaga, P.; Timmerman, H.; Leurs, R. Identification of 4-(1H-Imidazol-4(5)-ylmethyl)pyridine (immethridine) as a novel, potent, and highly selective histamine H₃ receptor agonist. *J. Med. Chem.* **2004**, *47*, 2414−2417.

(15) Meier, G.; Krause, M.; Hüls, A.; Ligneau, X.; Pertz, H. H.; Arrang, J. M.; Ganellin, C. R.; Schwartz, J. C.; Schunack, W.; Stark, H. 4-(ω-(Alkyloxy)alkyl)-1H-imidazole derivatives as histamine H₃ receptor antagonists/agonists. *J. Med. Chem.* **2004**, *47*, 2678−2687.

(16) Pelloux-Léon, N.; Fkyerat, A.; Piripitsi, A.; Tertiuk, W.; Schunack, W.; Stark, H.; Garbarg, M.; Ligneau, X.; Arrang, J.-M.; Schwartz, J.-C.; Ganellin, C. R. Meta-substituted aryl(thio)ethers as potent partial agonists (or antagonists) for the histamine H₃ receptor lacking a nitrogen atom in the side chain. *J. Med. Chem.* **2004**, *47*, 3264−3274.

(17) Kitbunnadaj, R.; Hashimoto, T.; Poli, E.; Zuiderveld, O. P.; Menozzi, A.; Hidaka, R.; de Esch, I. J. P.; Bakker, R. A.; Menge, W. M. P. B.; Yamatodani, A.; Coruzzi, G.; Timmerman, H.; Leurs, R. N-Substituted Piperidinyl Alkyl Imidazoles: Discovery of methimepip as a potent and selective histamine H₃ receptor agonist. *J. Med. Chem.* **2005**, *48*, 2100−2107.

(18) Govoni, M.; Lim, H. D.; El-Atmioui, D.; Menge, W. M. P. B.; Timmerman, H.; Bakker, R. A.; Leurs, R.; de Esch, I. J. P. A chemical switch for the modulation of the functional activity of higher homologues of histamine on the human histamine H₃ receptor: effect

of various substitutions at the primary amino function. *J. Med. Chem.* **2006**, *49*, 2549−2557.

(19) Wijtmans, M.; Celanire, S.; Snip, E.; Gillard, M. R.; Gelens, E.; Collart, P. P.; Venhuis, B. J.; Christophe, B.; Hulscher, S.; van der Goot, H.; Lebon, F.; Timmerman, H.; Bakker, R. A.; Lallemand, B. I. L. F.; Leurs, R.; Talaga, P. E.; de Esch, I. J. P. 4-Benzyl-1H-imidazoles with oxazoline termini as histamine H$_3$ receptor agonists. *J. Med. Chem.* **2008**, *51*, 2944−2953.

(20) Ishikawa, M.; Furuuchi, T.; Yamauchi, M.; Yokoyama, F.; Kakui, N.; Sato, Y. Synthesis and structure-activity relationships of N-aryl-piperidine derivatives as potent (partial) agonists for human histamine H$_3$ receptor. *Bioorg. Med. Chem.* **2010**, *18*, 5441−5448.

(21) Ishikawa, M.; Shinei, R.; Yokoyama, F.; Yamauchi, M.; Oyama, M.; Okuma, K.; Nagayama, T.; Kato, K.; Kakui, N.; Sato, Y. Role of hydrophobic substituents on the terminal nitrogen of histamine in receptor binding and agonist activity: development of an orally active histamine type 3 receptor agonist and evaluation of its antistress activity in mice. *J. Med. Chem.* **2010**, *53*, 3840−3844.

(22) Ishikawa, M.; Yamauchi, M.; Yokoyama, F.; Kudo, T.; Sato, Y.; Kakui, N.; Kato, K.; Watanabe, T. Investigation of the histamine H$_3$ receptor binding site. Design and synthesis of hybrid agonists with a lipophilic side chain. *J. Med. Chem.* **2010**, *53*, 6445−6456.

(23) Cannon, K. E.; Nalwalk, J. W.; Stadel, R.; Ge, P.; Lawson, D.; Silos-Santiago, I.; Hough, L. B. Activation of spinal histamine H$_3$ receptors inhibits mechanical nociception. *Eur. J. Pharmacol.* **2003**, *470*, 139−147.

(24) Yoshimoto, R.; Miyamoto, Y.; Shimamura, K.; Ishihara, A.; Takahashi, K.; Kotani, H.; Chen, A. S.; Chen, H. Y.; MacNeil, D. J.; Kanatani, A.; Tokita, S. Therapeutic potential of histamine H$_3$ receptor agonist for the treatment of obesity and diabetes mellitus. *Proc. Natl. Acad. Sci. U.S.A.* **2006**, *103*, 13866−13871.

(25) Reid, A. C.; Brazin, J. A.; Morrey, C.; Silver, R. B.; Levi, R. Targeting Cardiac Mast Cells: Pharmacological modulation of the local renin-angiotensin system. *Curr. Pharm. Des.* **2011**, *17*, 3744−3752.

(26) Hashikawa-Hobara, N.; Chan, N. Y.-K.; Levi, R. Histamine 3 receptor activation reduces the expression of neuronal angiotensin II type 1 receptors in the heart. *J. Pharmacol. Exp. Ther.* **2012**, *340*, 185−191.

(27) Lim, H. D.; Smits, R. A.; Bakker, R. A.; van Dam, C. M. E.; de Esch, I. J. P.; Leurs, R. Discovery of S-(2-Guanidylethyl)-isothiourea (VUF 8430) as a potent nonimidazole histamine H4 receptor agonist. *J. Med. Chem.* **2006**, *49*, 6650−6651.

(28) Leurs, R.; Smit, M. J.; Timmerman, H. Molecular Pharmacological Aspects of Histamine Receptors. *Pharmacol. Ther.* **1995**, *66*, 413−463.

(29) van der Goot, H.; Eriks, J. C.; Leurs, R.; Timmerman, H. Amselamine, a new selective histamine H$_2$-receptor agonist. *Bioorg. Med. Chem. Lett.* **1994**, *4*, 1913−1916.

(30) Kushida, N.; Watanabe, N.; Okuda, T.; Yokoyama, F.; Gyobu, Y.; Yaguchi, T. PF1270A, B and C, novel histamine H3 receptor ligands produced by *Penicillium waksmanii* PF1270. *J. Antibiot.* **2007**, *60*, 667−673.

(31) Shi, Y.; Sheng, R.; Zhong, T.; Xu, Y.; Chen, X.; Yang, D.; Sun, Y.; Yang, F.; Hu, Y.; Zhou, N. Identification and characterization of ZEL-H16 as a novel agonist of the histamine H$_3$ receptor. *PLoS One* **2012**, *7*, No. e42185.

(32) Ghoshal, A.; Kumar, A.; Yugandhar, D.; Sona, C.; Kuriakose, S.; Nagesh, K.; Rashid, M.; Singh, S. K.; Wahajuddin, M.; Yadav, P. N.; Srivastava, A. K. Identification of novel β-lactams and pyrrolidinone derivatives as selective histamine-3 receptor (H3R) modulators as possible anti-obesity agents. *Eur. J. Med. Chem.* **2018**, *152*, 148−159.

(33) Igel, P.; Dove, S.; Buschauer, A. Histamine H$_4$ receptor agonists. *Bioorg. Med. Chem. Lett.* **2010**, *20*, 7191−7199.

(34) Geyer, R.; Kaske, M.; Baumeister, P.; Buschauer, A. Synthesis and functional characterization of imbutamine analogs as histamine H$_3$ and H$_4$ receptor ligands. *Arch. Pharm.* **2014**, *347*, 77−88.

(35) Kiss, R.; Keseru, G. M. Novel histamine H4 receptor ligands and their potential therapeutic applications: an update. *Expert Opin. Ther. Pat.* **2014**, *24*, 1−13.

(36) Black, L. A.; Gfesser, G. A.; Cowart, M. D. 4-Substituted-2-amino-pyrimidine Derivatives. US20100331294, 2010.

(37) Carceller González, E.; Medina Fuentes, E. M.; Martí Via, J.; Virgili Barnardó, M. 2-Amino-pyrimidine Derivatives as Histamine H$_4$ Antagonists. WO2009068512, 2009.

(38) Cai, H.; Chavez, F.; Edwards, J. P.; Fitzgerald, A. E.; Liu, J.; Mani, N. S.; Neff, D. K.; Rizzolio, M. C.; Savall, B. M.; Smith, D. M.; Venable, J. D.; Jianmei, W.; Wolin, R. 2-Aminopyrimidine Modulators of the Histamine H$_4$ Receptor. WO2008100565, 2010.

(39) Sassano, M. F.; Doak, A. K.; Roth, B. L.; Shoichet, B. K. Colloidal aggregation causes inhibition of G protein-coupled receptors. *J. Med. Chem.* **2013**, *56*, 2406−2414.

(40) Sirci, F.; Istyastono, E. P.; Vischer, H. F.; Kooistra, A. J.; Nijmeijer, S.; Kuijer, M.; Wijtmans, M.; Mannhold, R.; Leurs, R.; de Esch, I. J. P.; de Graaf, C. Virtual fragment screening: Discovery of histamine H$_3$ receptor ligands using ligand-based and protein-based molecular fingerprints. *J. Chem. Inf. Model.* **2012**, *52*, 3308−3324.

(41) Kooistra, A. J.; Kuhne, S.; de Esch, I. J. P.; Leurs, R.; de Graaf, C. A structural chemogenomics analysis of aminergic GPCRs: Lessons for histamine receptor ligand design. *Br. J. Pharmacol.* **2013**, *170*, 101−126.

(42) Jongejan, A.; Lim, H. D.; Smits, R. A.; de Esch, I. J. P.; Haaksma, E.; Leurs, R. Delineation of agonist binding to the human histamine H$_4$ receptor using mutational analysis, homology modeling, and ab initio calculations. *J. Chem. Inf. Model.* **2008**, *48*, 1455−1463.

(43) Shin, N.; Coates, E.; Murgolo, N. J.; Morse, K. L.; Bayne, M.; Strader, C. D.; Monsma, F. J. Molecular modeling and site-specific mutagenesis of the histamine-binding site of the histamine H$_4$ receptor. *Mol. Pharmacol.* **2002**, *62*, 38−47.

(44) Istyastono, E. P.; Nijmeijer, S.; Lim, H. D.; Stolpe van de, A.; Roumen, L.; Kooistra, A. J.; Vischer, H. F.; de Esch, I. J. P.; Leurs, R.; de Graaf, C. Molecular determinants of ligand binding modes in the histamine H$_4$ receptor: linking ligand-based three-dimensional quantitative structure−activity relationship (3D-QSAR) models to in silico guided receptor mutagenesis studies. *J. Med. Chem.* **2011**, *54*, 8136−8147.

(45) Uveges, A. J.; Kowal, D.; Zhang, Y.; Spangler, T. B.; Dunlop, J.; Semus, S.; Philip, G. J. The role of transmembrane helix 5 in agonist binding to the human H$_3$ receptor. *J. Pharmacol. Exp. Ther.* **2002**, *301*, 451−458.

(46) Shimamura, T.; Shiroishi, M.; Weyand, S.; Tsujimoto, H.; Winter, G.; Katritch, V.; Abagyan, R.; Cherezov, V.; Liu, W.; Han, G. W.; Kobayashi, T.; Stevens, R. C.; Iwata, S. Structure of the human histamine H1 receptor complex with doxepin. *Nature* **2011**, *475*, 65−72.

(47) Morse, K. L.; Behan, J.; Laz, T. M.; West, R. E. J.; Greenfeder, S. A.; Anthes, J. C.; Umland, S.; Wan, Y.; Hipkin, R. W.; Gonsiorek, W.; Shin, N.; Gustafson, E. L.; Qiao, X.; Wang, S.; Hedrick, J. A.; Greene, J.; Bayne, M.; Monsma, F. J. J. Cloning and characterization of a novel human histamine receptor. *J. Pharmacol. Exp. Ther.* **2001**, *269*, 1058−1066 https://www.ncbi.nlm.nih.gov/pubmed/11181941.

(48) Obach, R. S. Prediction of human clearance of twenty-nine drugs from hepatic microsomal intrinsic clearance data: An examination of in vitro half-life approach and nonspecific binding to microsomes. *Drug Metab. Dispos.* **1999**, *27*, 1350−1359 https://www.ncbi.nlm.nih.gov/pubmed/10534321.

(49) Lin, J. H.; Lu, A. Y. H. Inhibition and induction of cytochrome P450 and the clinical implications. *Clin. Pharmacokinet.* **1998**, *35*, 361−390.

(50) Provensi, G.; Costa, A.; Izquierdo, I.; Blandina, P.; Passani, M. B. Brain histamine modulates recognition memory: possible implications in major cognitive disorders. *Br. J. Pharmacol.* **2018**, DOI: 10.1111/bph.14478.

(51) Prast, H.; Argyriou, A.; Philippu, A. Histaminergic neurons facilitate social memory in rats. *Brain Res.* **1996**, *734*, 316−318.

(52) Provensi, G.; Passani, M. B.; Costa, A.; Izquierdo, I.; Blandina, P. Neuronal histamine and the memory of emotionally salient events. *Br. J. Pharmacol.* **2018**, DOI: 10.1111/bph.14476.

(53) Parmentier, R.; Anaclet, C.; Guhennec, C.; Brousseau, E.; Bricout, D.; Giboulot, T.; Bozyczko-Coyne, D.; Spiegel, K.; Ohtsu, H.; Williams, M.; Lin, J. S. The brain H_3-receptor as a novel therapeutic target for vigilance and sleep-wake disorders. *Biochem. Pharmacol.* **2007**, *73*, 1157−1171.

(54) Yokoyama, F.; Yamauchi, M.; Oyama, M.; Okuma, K.; Onozawa, K.; Nagayama, T.; Shinei, R.; Ishikawa, M.; Sato, Y.; Kakui, N. Anxiolytic-like profiles of histamine H_3 receptor agonists in animal models of anxiety: a comparative study with antidepressants and benzodiazepine anxiolytic. *Psychopharmacology* **2009**, *205*, 177−187.

(55) Schneider, E. H.; Neumann, D.; Seifert, R. Histamine H_4-receptor expression in the brain? *Naunyn-Schmiedeberg's Arch. Pharmacol.* **2015**, *388*, 5−9.

(56) Sanna, M. D.; Ghelardini, C.; Thurmond, R. L.; Masini, E.; Galeotti, N. Behavioural phenotype of histamine H_4 receptor knockout mice: Focus on central neuronal functions. *Neuropharmacology* **2017**, *114*, 48−57.

(57) Blandina, P.; Giorgetti, M.; Bartolini, L.; Cecchi, M.; Timmerman, H.; Leurs, R.; Pepeu, G.; Giovannini, M. G. Inhibition of cortical acetylcholine release and cognitive performance by histamine H_3 receptor activation in rats. *Br. J. Pharmacol.* **1996**, *119*, 1656−1664.

(58) Nijmeijer, S.; Engelhardt, H.; Schultes, S.; van de Stolpe, A. C.; Lusink, V.; de Graaf, C.; Wijtmans, M.; Haaksma, E. E. J.; de Esch, I. J. P.; Stachurski, K.; Vischer, H. F.; Leurs, R. Design and pharmacological characterization of VUF14480, a covalent partial agonist that interacts with cysteine $98^{3.36}$ of the human histamine H_4 receptor. *Br. J. Pharmacol.* **2013**, *170*, 89−100.

(59) Mocking, T. A. M.; Verweij, E. W. E.; Vischer, H. F.; Leurs, R. Homogeneous, real-time NanoBRET binding assays for the histamine H_3 and H_4 receptors on living cells. *Mol. Pharmacol.* **2018**, *94*, 1371−1381.

(60) Hauwert, N. J.; Mocking, T. A. M.; Da Costa Pereira, D.; Lion, K.; Huppelschoten, Y.; Vischer, H. F.; de Esch, I. J. P.; Wijtmans, M.; Leurs, R. A photoswitchable agonist for the histamine H_3 receptor, a prototypic family a G-protein-coupled receptor. *Angew. Chem., Int. Ed.* **2019**, *58*, 4531−4535.

(61) Cheng, Y.-C.; Prusoff, W. H. Relation between the inhibition constant (Ki) and the concentration of inhibitor which causes 50 percent inhibiton (IC50) of an enzymatic reaction. *Biochem. Pharmacol.* **1973**, *22*, 3099−3108.

(62) Huang, Z.; Li, H.; Zhang, Q.; Tan, X.; Lu, F.; Liu, H.; Li, S. Characterization of preclinical in vitro and in vivo pharmacokinetics properties for KBP-7018, a new tyrosine kinase inhibitor candidate for treatment of idiopathic pulmonary fibrosis. *Drug Des., Dev. Ther.* **2015**, *9*, 4319−4328.

(63) Smith, R.; Jones, R. D. O.; Ballard, P. G.; Griffiths, H. H. Determination of microsome and hepatocyte scaling factors for in vitro/in vivo extrapolation in the rat and dog. *Xenobiotica* **2008**, *38*, 1386−1398.

(64) Isberg, V.; de Graaf, C.; Bortolato, A.; Cherezov, V.; Katritch, V.; Marshall, F. H.; Mordalski, S.; Pin, J.-P.; Stevens, R. C.; Vriend, G.; Gloriam, D. E. Generic GPCR residue numbers - aligning topology maps minding the gaps. *Trends Pharmacol. Sci.* **2015**, *36*, 22−31.

(65) Sali, A. Comparative protein modeling by satisfaction of spatial restraints. *Mol. Med. Today* **1995**, *1*, 270−277.

(66) Bateman, A.; Martin, M. J.; O'Donovan, C.; Magrane, M.; Alpi, E.; Antunes, R.; Bely, B.; Bingley, M.; Bonilla, C.; Britto, R.; Bursteinas, B.; Bye-AJee, H.; Cowley, A.; Da Silva, A.; De Giorgi, M.; Dogan, T.; Fazzini, F.; Castro, L. G.; Figueira, L.; Garmiri, P.; Georghiou, G.; Gonzalez, D.; Hatton-Ellis, E.; Li, W.; Liu, W.; Lopez, R.; Luo, J.; Lussi, Y.; MacDougall, A.; Nightingale, A.; Palka, B.; Pichler, K.; Poggioli, D.; Pundir, S.; Pureza, L.; Qi, G.; Rosanoff, S.; Saidi, R.; Sawford, T.; Shypitsyna, A.; Speretta, E.; Turner, E.; Tyagi, N.; Volynkin, V.; Wardell, T.; Warner, K.; Watkins, X.; Zaru, R.; Zellner, H.; Xenarios, I.; Bougueleret, L.; Bridge, A.; Poux, S.; Redaschi, N.; Aimo, L.; ArgoudPuy, G.; Auchincloss, A.; Axelsen, K.; Bansal, P.; Baratin, D.; Blatter, M. C.; Boeckmann, B.; Bolleman, J.; Boutet, E.; Breuza, L.; Casal-Casas, C.; De Castro, E.; Coudert, E.; Cuche, B.; Doche, M.; Dornevil, D.; Duvaud, S.; Estreicher, A.; Famiglietti, L.; Feuermann, M.; Gasteiger, E.; Gehant, S.; Gerritsen, V.; Gos, A.; Gruaz-Gumowski, N.; Hinz, U.; Hulo, C.; Jungo, F.; Keller, G.; Lara, V.; Lemercier, P.; Lieberherr, D.; Lombardot, T.; Martin, X.; Masson, P.; Morgat, A.; Neto, T.; Nouspikel, N.; Paesano, S.; Pedruzzi, I.; Pilbout, S.; Pozzato, M.; Pruess, M.; Rivoire, C.; Roechert, B.; Schneider, M.; Sigrist, C.; Sonesson, K.; Staehli, S.; Stutz, A.; Sundaram, S.; Tognolli, M.; Verbregue, L.; Veuthey, A. L.; Wu, C. H.; Arighi, C. N.; Arminski, L.; Chen, C.; Chen, Y.; Garavelli, J. S.; Huang, H.; Laiho, K.; McGarvey, P.; Natale, D. A.; Ross, K.; Vinayaka, C. R.; Wang, Q.; Wang, Y.; Yeh, L. S.; Zhang, J. UniProt: The universal protein knowledgebase. *Nucleic Acids Res.* **2017**, *45*, D158−D169.

(67) Sadowski, J.; Gasteiger, J.; Klebe, G. Comparison of automatic three-dimensional model builders using 639 X-ray structures. *J. Chem. Inf. Model.* **1994**, *34*, 1000−1008.

(68) ChemAxon, L.. *Calculator*; ChemAxon: Budapest, Hungary, 1998−2018.

(69) Korb, O.; Stützle, T.; Exner, T. E. An ant colony optimization approach to flexible protein−ligand docking. *Swarm Intell.* **2007**, *1*, 115−134.

(70) Marcou, G.; Rognan, D. Optimizing fragment and scaffold docking by use of molecular interaction fingerprints. *J. Chem. Inf. Model.* **2007**, *47*, 195−207.

(71) de Graaf, C.; Kooistra, A. J.; Vischer, H. F.; Katritch, V.; Kuijer, M.; Shiroishi, M.; Iwata, S.; Shimamura, T.; Stevens, R. C.; de Esch, I. J. P.; Leurs, R. Crystal structure-based virtual screening for fragment-like ligands of the human histamine H_1 receptor. *J. Med. Chem.* **2011**, *54*, 8195−8206.

(72) Jakalian, A.; Jack, D. B.; Bayly, C. I. Fast, efficient generation of high-quality atomic charges. AM1-BCC model: II. Parameterization and validation. *J. Comput. Chem.* **2002**, *23*, 1623−1641.

(73) Berendsen, H. J. C.; van der Spoel, D.; van Drunen, R. GROMACS: A message-passing parallel molecular dynamics implementation. *Comput. Phys. Commun.* **1995**, *91*, 43−56.

(74) Cordomí, A.; Caltabiano, G.; Pardo, L. Membrane protein simulations using AMBER force field and Berger lipid parameters. *J. Chem. Theory Comput.* **2012**, *8*, 948−958.

(75) Roessler, W. G.; Brewer, C. R. Permanent turbidity standards. *Appl. Microbiol.* **1967**, *15*, 1114−1121.

(76) Baell, J. B.; Holloway, G. A. New substructure filters for removal of pan assay interference compounds (PAINS) from screening libraries and for their exclusion in bioassays. *J. Med. Chem.* **2010**, *53*, 2719−2740.